EIT KIC InnoEnergy Master's Programme

Renewable Energy - RENE

MSc Thesis

Study of the shading effects on photovoltaic (PV) modules in building integrated photovoltaics (BIPV)

Author: Denis Ariho

Supervisors:

Principal supervisor: Santiago Silvestre/UPC

Industrial supervisor: Nuria Martín Chivelet/CIEMAT

Session: September 2013

Escola Tècnica Superior d'Enginyeria Industrial de Barcelona
UNIVERSITAT POLITÈCNICA DE CATALUNYA

MSc RENE is a cooperation between

Universitat Politècnica de Catalunya, Spain │ KTH-Royal Institute of Technology, Sweden
Instituto Superior Técnico, Portugal │ École Polytechnique (ParisTech), France

ACKNOWLEDGEMENTS

I express my special thanks to the Almighty God for the gift of life and for granting me the strength to work on this thesis work.

My since thanks go the administration of CIEMAT in Madrid, Spain who gave me an opportunity to do the thesis and internship in their institution. I greatly thank Madam Nuria Martin Chivelet, my supevisor at CIEMAT for working tirelessly to make sure I get all the information needed and reviewing my thesis work to match with the required standards. I thank employees of CIEMAT who directly or indirectly were responsible for my stay at CIEMAT: Enrique Soria (Director Renewable Energy Division), Faustino Chenlo (Head of Solar department), Eduardo Mejuto, M. Carmen Del Alonso Garcia, Jose Domingo, Felix Santiago Garcia Rosillo, Jose Cuenca, Filipe Soriano, Sergio Temprano, Antonio Leal, Nieves Vela, Fernando Fabero.

I thank Associate Prof. Santiago Silvestre, my academic supervisor at Universitat Politecnica de Catalunya (UPC) in Barcelona, Spain who guided me in the thesis work approach, gave me all requirement information and for reviewing thesis work to match with the required standards.

I also thank the administration of Instituto Superior Tecnico (IST) in Lisbon, Portugal and Universitat Politecnica de Catalunya (UPC) for granting me the education skills to approach the thesis work.

I cannot forget to thank my funders of the masters' programme; Knowledge Innovation Communities (KIC) Inno-energy and European Institute of Innovation and Technology (EIT). Without your support, i would not have managed to study this masters programme.

May the Almighty God bless you abundantly in your lives and plans.

DEDICATION

This work is dedicated to my parents Mr and Mrs Pontious Turyahabwa for their parenthood, support and direction in my life.

I also dedicate this work to my brothers, sisters, friends, relatives and every one who has contributed directly or indirectly to my education. Special thanks to Nansumba Hellen for her continued prayers, encouragement and advice.

I also dedicate this thesis work to some friends for their encouragement as I compiled this report: S.M. Safayet Ullah, Thewodros Nigusse and Mulugeta Ayele.

May the Almighty God bless you abundantly.

ABSTRACT

This thesis work focuses on the effect of shading on the photovoltaic (PV) modules in building integrated photovoltaics (BIPV). The main objective of this thesis work is to analyse and characterise the electrical and thermal behaviour of the PV modules when they are partially shaded, a circumstance which frequently occurs in photovoltaic installations in buildings. The PV module technologies considered in this research are; Cadmium Telluride (CdTe), Copper Indium Selenide (CIS), amorphous silicon heterojunction, amorphous silicon simple junction, amorphous silicon triple junction, mono-crystalline silicon (Kyocera), mono-crystalline silicon (Suntech), mono-crystalline silicon back contacts and multi-crystalline silicon (Si-mc). The electrical and thermal measurements were done in outdoor conditions to obtain data in real operating conditions.

Each PV module technology was exposed to different shadow patterns and the I-V curves measured. In order to correct the measured I-V curves to the same testing conditions, the IEC 60904-1 standard was considered, in which it is necessary to know the values of the temperature coefficients, internal series resistance (R_s) and curve correction factor (k).

The shadow patterns resulted into the reduction of the electrical characteristics (current, voltage and power) for each module technology. The shading also resulted into the reduction of the maximum power of each module technology and there were no hot spots in the modules. The magnitude of the electrical parameters of the PV module technologies due to shading depends on the shadow patterns, arrangement of the cells and location of bypass diodes in the modules. The thermal characterisation indicates that shading resulted into the reduction of the module temperatures in comparison to the unshaded module and there were no hot spots in all the module technologies. Therefore, all the module technologies tested are capable of being applied in building integrated photovoltaics (BIPV) since they are not affected by hot spot phenomena in the real operating conditions.

The comparison of the different PV module technologies with the same shadow patterns indicates that the PV modules perform differently with shading. The results indicate that some PV module technologies which perform well in one shadow type do not perform well in another shadow type. In the application of BIPV in buildings, shading should be taken as a priority since it greatly affects the electrical and thermal characteristics of the modules. The nature of the shadows in a location should be considered before selecting the PV module technologies to apply in the BIPV system.

TABLE OF CONTENTS

1. GLOSSARY

DC: Direct current

AC: Alternating current

PV: Photovoltaics

BIPV: Building integrated photovoltaics

MPP: Maximum power point

CdTe: Cadmium Telluride

CIS: Copper Indium Selenide

a-Si: Amorphous silicon

m-Si: Mono-crystalline silicon

mc-Si: Multi-crystalline silicon

USA: United States of America

$\mathbf{V_{mp}}$: Voltage at maximum power

$\mathbf{I_{mp}}$: Current at maximum power

$\mathbf{V_{oc}}$: Open circuit voltage

$\mathbf{I_{sc}}$: Short circuit current

HIT: Heterojunction with Intrinsic Thin Layer

InP: Indium Phosphide

GaSb: Gallium antimony

GaAs: Gallium arsenide

Ge: Germanium

GaInP: Indium gallium phosphide

CIGS: Copper Indium Gallium Selenide

I-V: Current versus voltage

SRC: Standard reporting conditions

MPPT: Maximum power point tracking

STC: Standard test conditions

NOCT: Normal operating cell temperature

IR: Infrared

$\mathbf{R_s}$: Internal series resistance

k: Curve correction factor

α: Current temperature coefficient

β: Voltage temperature coefficient

γ: Power temperature coefficient

$\mathbf{J_m}$: Maximum current density

$\mathbf{J_{sc}}$: Short circuit current density

2. PREFACE

Photovoltaics (PV) is the production of Direct current (DC) when the semi-conductor devices called solar cells are illuminated by photons from the sun's solar radiation. The DC is converted to alternating current (DC) by inverters. The PV systems can be applied in stand-alone and grid connected systems. The prices of photovoltaics have gradually decreased and this has made investment in the solar projects become financially attractive for governments, manufacturing companies, investors and home users.

The installation of photovoltaic systems requires a large area which may compete with the area available for agricultural, industrial and recreational purposes. Therefore, buildings should be modified to generate energy through building integrated photovoltaics (BIPV). Building Integrated Photovoltaics (BIPV) is the use of Photovoltaics (PV) as a part of the structure of the building especially in the roofing and facades. The surrounding environment should be taken into consideration before the installation of the BIPV system because any partial shades on the photovoltaic modules caused by the adjacent structures or trees may deteriorate the performance of the system. There are many factors which may cause the reduction of the output power in photovoltaic modules but the most important include; shadows and maximum power point MPP) mismatch.

The main objective of this work is to analyse and characterise the electrical and thermal behaviour of the PV modules when they are partially shaded, a circumstance which frequently occurs in photovoltaic installations in buildings. The PV module technologies considered in this research are; Cadmium Telluride (CdTe), Copper Indium Selenide (CIS), amorphous silicon heterojunction, amorphous silicon simple junction, amorphous silicon triple junction, mono-crystalline silicon (Kyocera), mono-crystalline silicon (Suntech), mono-crystalline silicon back contacts and multi-crystalline silicon (Si-mc).

The electrical and thermal measurements were done in outdoor conditions to obtain data in real operating conditions. The PV modules were subjected to different shadow patterns and the electrical and thermal characteristics were obtained. The shadow patterns resulted into the reduction of the electrical characteristics (current, voltage and power) for each module technology. The shading also resulted into the reduction of the maximum power of each module technology and there were no hot spots in the modules. The comparison of the different PV module technologies with the same shadow patterns indicates that the PV modules perform differently with shading.

3. INTRODUCTION

Photovoltaics refers to the production of Direct current (DC) when the semi-conductor devices called solar cells are illuminated by photons from the sun's solar radiation. The photovoltaic systems contain inverters that transform the DC current to Alternating current (AC) to supply the AC loads. The DC and AC currents supply the DC and AC loads respectively.

Photovoltaics is currently seen as a smart technology which can be used to transform buildings into contemporary energy generators [1]. Architects are currently very interested in renewable energy systems especially those that can be used to reduce the energy bill of buildings. There has been an increasing trend in the adoption of renewable energies due to the increase in the prices of oil products and increase in the greenhouse gases in the Earth's atmosphere.

The prices of photovoltaics have gradually decreased and this has made investment in the solar projects become financially attractive for governments, manufacturing companies, investors and home users. Over the last 20 years, the prices of PV modules have decreased by over 20% every time the cumulative sold volume of the PV modules has doubled and in the last 5 years in Europe, the prices of PV modules have decreased by 50% [2]. PV system prices are also expected to decrease in the coming 10 years by 31-50% depending on the segment and the generation costs are expected to decrease by 50% by 2020. The cost of PV electricity generation in Europe could decrease from 0.16-0.35 €/kWh in 2010 to 0.08-0.18 €/kWh in 2020 depending on the system size and irradiance level.

Building Integrated Photovoltaics (BIPV) is the use of Photovoltaics (PV) as a part of the structure of the building especially in the roofing and facades [3]. The surrounding environment should be taken into consideration before the installation of the BIPV system because any partial shades on the photovoltaic modules caused by the adjacent structures or trees may deteriorate the performance of the system.

There are many factors which can cause the reduction of the output power in photovoltaic modules but the most important include; shadows and maximum power point MPP) mismatch. If the PV module is partially shaded, some of its cells may work in a reverse bias. When the reverse bias voltage exceeds the break down voltage of the shaded solar cell, the solar cell may get fully damaged for example hot spot formation appears, cell cracking and an open circuit exists at the serial branch where the cell is connected [4]. The partial shading in PV modules results into electrical and thermal effects. The partial shading of the

photovoltaic modules may become the main cause of power losses in PV installations [5].

In most PV modules on the market, the solar cells are connected in series and have bypass diodes to avoid hot spot phenomena. Commercial PV modules usually have a diode for every 18 to 20 solar cells [5]. The electrical configuration of the PV module, the number and position of the solar cells associated to each bypass diode determine the characteristic I-V curve of the PV module for every shadow pattern.

The shadow pattern and PV module configuration greatly affect the electrical and thermal characteristics. There are also other factors which contribute to the electrical and thermal effects include irradiance level, clearness index and ambient temperature [5].

In this work, the effect of shading on the PV modules in BIPV was analysed by determining the electrical and thermal characterisation of the PV modules when subjected to different shading patterns. The experiments were done on 9 PV modules of different technologies and from different manufacturers. The PV modules tested include: Cadmium Telluride (CdTe), Copper Indium Selenide (CIS), amorphous silicon heterojunction, amorphous silicon simple junction, amorphous silicon triple junction, mono-crystalline silicon (Kyocera), mono-crystalline silicon (Suntech), mono-crystalline silicon back contacts and multi-crystalline silicon (Si-mc).

Objectives

Main objective

To analyse and characterise the electrical and thermal behaviour of the PV modules when they are partially shaded, a circumstance which frequently occurs in photovoltaic installations in buildings.

Specific objectives

- To know the influence of the setting, the type of technology and the module layout in their behaviour.
- To analyze the influence of the behaviour of each module in the durability of the facilities.

4. LITERATURE REVIEW

4.1 Fundamentals of photovoltaics (PV)

Photovoltaics (PV) is the production of Direct current (DC) electricity when the semi-conductor devices called photovoltaic solar cells are illuminated by photons from the sun's radiation [3]. The history of Photovoltaics begins in the 19th century and the first commercial use of solar cells started in 1958. During that period, the United States of America (USA) and U.S.S.R space programmes were using solar cells for powering satellites and this was the main commercial application of solar until 1970. The support for photovoltaics has been increasing in several European countries such as Italy, The Netherlands, Spain, Switzerland, Austria, and Finland [23]. The photovoltaic technology has a variety of applications ranging in power from a few microwatts to tens of megawatts such as pocket calculators, small residential houses, and solar water pumps.

Basics of the photovoltaic cell
The photovoltaic cell is an electrical device that converts the energy of photons from the solar radiation to electricity by photovoltaic effect. A photon in the solar cell can generate an electron-hole pair if it has the energy greater than the band gap.

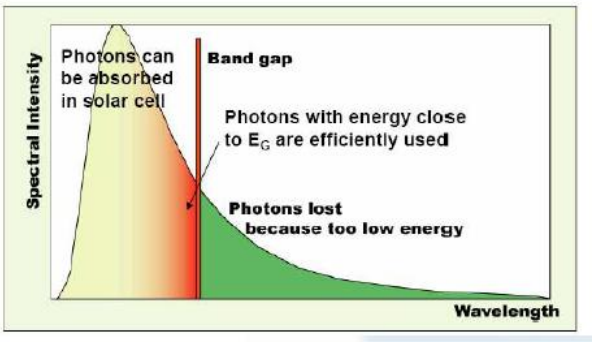

Fig. 4.1. Effect of band gap on the photon absorption

The PV cells have the current-voltage characteristics when exposed to sun's radiation. When the solar cells are exposed to dark conditions, they behave to have the diode current-voltage characteristics.

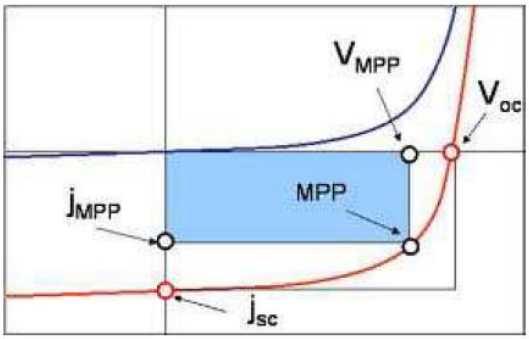

Fig. 4.2. I-V characteristics of the PV cell when exposed to dark and light conditions

The blue and red curves show the current-voltage characteristics in dark and light conditions respectively.
I-V curves have the open circuit voltage (V_{oc}), short circuit current density (j_{sc}), current at maximum power (j_{mpp}). The open circuit voltage (V_{oc}) is the voltage at which no current flows through the PV cell. It is also referred to a point at which the photo current generation and dark current coincide. Short circuit current density (j_{sc}) is the current density at which there is no voltage across the solar cell.

Fill factor
The fill factor is the ratio between the maximum power of the PV cell to the potential power. It is very necessary in determining the performance of solar cells.

$$FF = \frac{J_{mpp}V_{mpp}}{J_{sc}V_{oc}} \quad (1)$$

Where;
J_{mpp}-current density at maximum power
V_{mp}-voltage at maximum power
J_{sc}-Short circuit current density

Efficiency
Efficiency is the ratio of the output power to the incident power on the solar cell.

$$\eta = \frac{J_{mpp}V_{mpp}}{P_0} = \frac{FF * J_{sc} * V_{oc}}{P_0} \quad (2)$$

Where; P_0 is the incident power

The solar cell circuit model

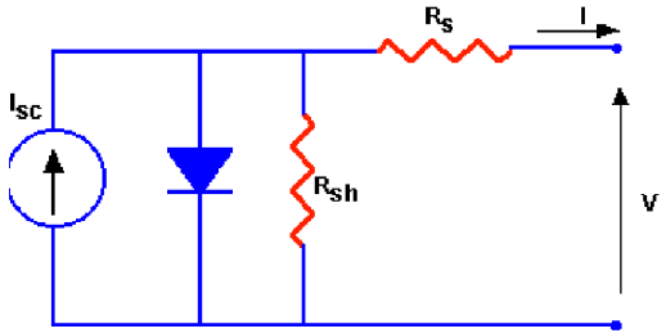

Fig. 4.3. Solar cell circuit model

The solar cell circuit model takes into account the parasitic losses of the series and shunt resistances.

Current technologies of photovoltaics

There are different types of photovoltaic solar cells and have different efficiencies. The photo-electrochemical process was first discovered by A. E. Becquerel in 1839 and from that period, there has been advancement in improving the efficiency of the solar cells. The efficiencies of the PV cells have been compiled in the figure below;

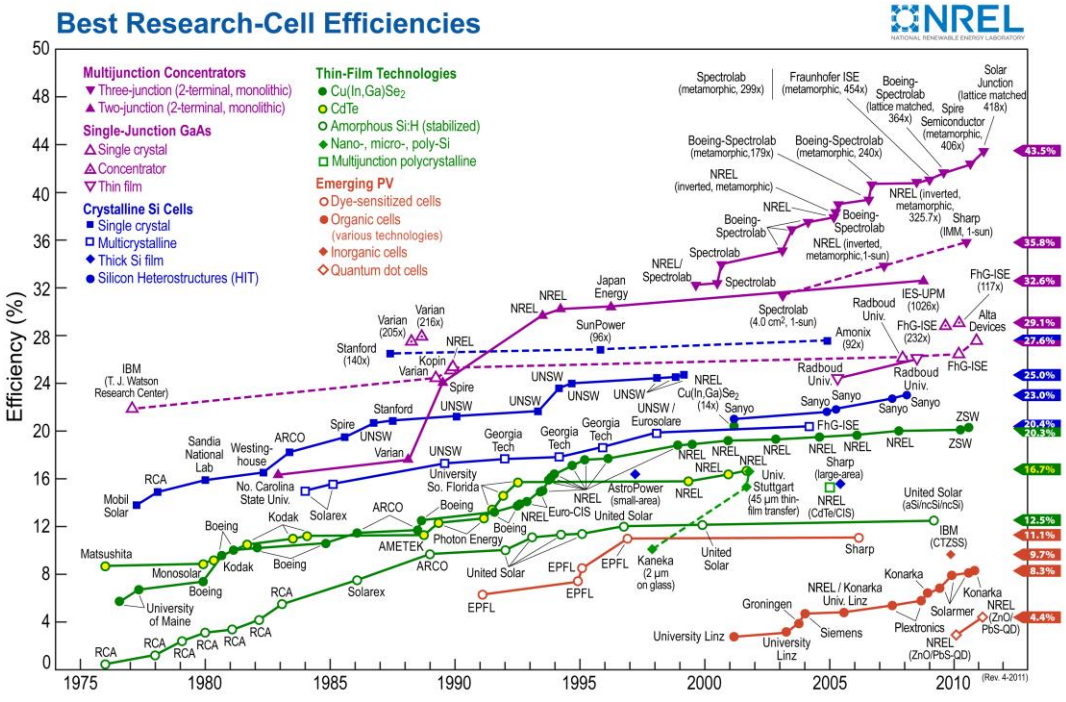

Fig. 4.4. Evolution of solar cell efficiencies [19]

4.2 Photovoltaic technologies

The main types of semiconductors used in the solar cells currently include; Mono and Muti-crystalline silicon, amorphous silicon, gallium arsenide (GaAs), copper-indium-deselenide ($CuInSe_2$), and cadmium telluride (CdTe) [23].

Crystalline silicon cells
Crystalline silicon solar cells are categorised into; mono-crystalline, multi-crystalline and Hetero-junction with Intrinsic Thin layer (HIT). Mono and multi-crystalline solar cells occupy about 85% of the market share. The modules have a life time of around 25-30 years at a minimum of 80% of the rated output. The maximum efficiency for mono crystalline silicon is 25%.The efficiency of crystalline silicon solar cells decreases with increasing temperature.

Another category of crystalline silicon solar cells is HIT (Hetero-junction with Intrinsic Thin layer) which is composed of a mono thin crystalline wafer surrounded by ultra-thin amorphous silicon layers. They improve boundary characteristics and reduce power losses by forming impurity free i-type amorphous silicon layers between the crystalline base, p and n type amorphous silicon layers. The HIT cells have achieved an efficiency of 24.7% by Panasonic. The higher efficiencies can be achieved by spectral splitting of light to optimize solar cells for a range of wavelengths [23]. This can be achieved in the following PV technologies; multi-junction, tandem or stacked cells.

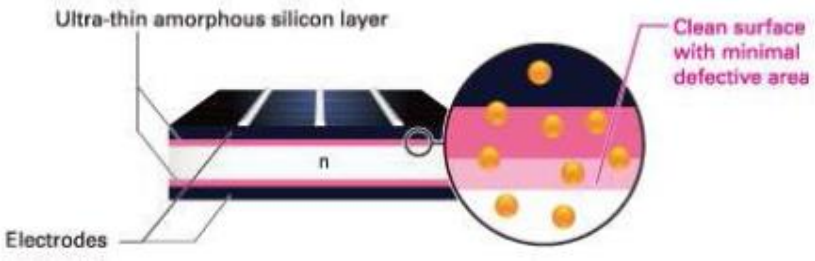

Fig. 4.5. Structure of HIT solar cell

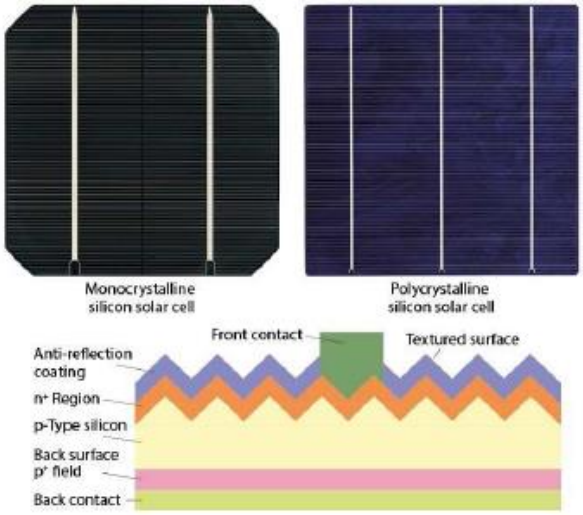

Fig. 4.6. View of mono-crystalline, multi-crystalline silicon solar cell and the structure of a textured crystalline solar cell (below)

Group III-IV solar cells

The most common Group III-IV solar cells are Indium phosphide (InP), gallium antimony (GaSb) and gallium arsenide (GaAs). The most commonly used solar cells are GaAs. Group III-IV solar cells have high cost and high efficiency.

GaAs, germanium (Ge) and indium gallium phosphide (GaInP) are used in the fabrication of multi-junction solar cells. The multi-junction solar cells have sub cells that absorb the solar radiation of different wave lengths and thus increasing the conversion efficiency as shown in figure 4.7. They have the highest conversion efficiency in the world so far and are mainly used in photovoltaic concentrator technology for power stations.

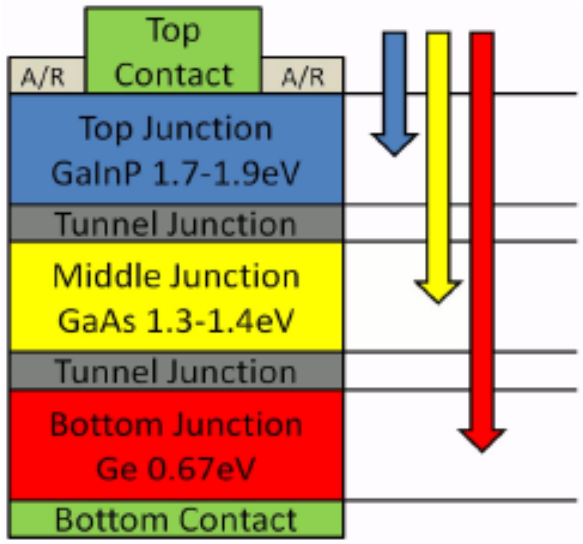

Fig. 4.7. Structure of multi-junction III-V solar cells

Thin film solar cells

Copper Indium Gallium Selenide (CIGS) solar cells

These solar cells highly absorb the solar radiation and are much thinner than other semi-conductor materials. It is possible to fabricate flexible solar modules since they are thin technologies. Flexible thin film solar cells have reached a record efficiency of 20.4% although in many cases are less efficient when compared to crystalline silicon solar cells.

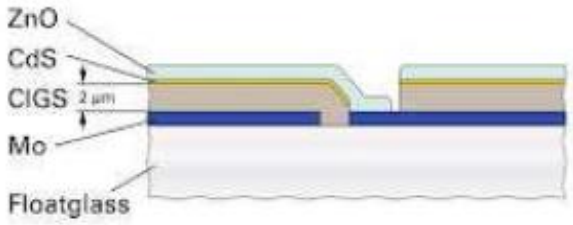

Fig. 4.8. Structure of CIGS solar cell

Cadmium Telluride (CdTe)

Cadmium telluride (CdTe) thin film solar cells have lower manufacturing costs when compared to silicon solar cells and other technologies. Cadmium is abundant but Telluride is not. Nevertheless cadmium is one of the most top toxic materials in the world so this fact must be taken into account in the manufacturing process and in the life cycle of these kinds of PV modules.

The best cell efficiency achieved so far by GE Global research in this type of modules is 18.3%. Cadmium telluride can absorb solar radiation with short wavelength which may not be achieved by silicon solar cells. Nevertheless they have lower efficiency than silicon solar cells.

Amorphous silicon (a-Si)

Amorphous silicon solar cells are mainly used in calculators, other small electronic devices and also in BIPV. They are produced by silicon deposition to a very thin layer and have lower efficiency than mono and multi-crystalline solar cells. The best efficiency reached by LG electronics is 13.4%. The amorphous silicon solar cells have lower expected life than crystalline solar cells.

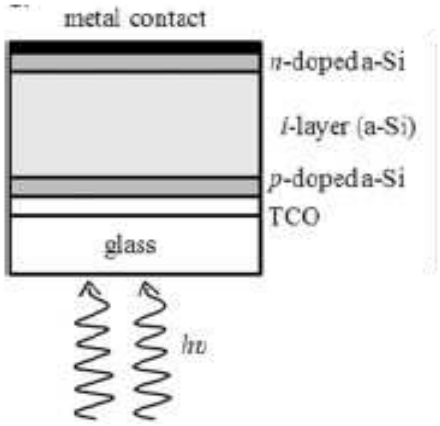

Fig. 4.9. Structure of amorphous silicon solar cell

3.3 Electrical Characterization of PV Devices

The performance of solar cells and modules is based on the current versus voltage (I-V) and spectral responsivity versus wavelength characteristics [6]. The performance indicator mainly considered in PV cells and modules is the PV efficiency under standard reporting conditions (SRC) such as temperature, spectral irradiance and total irradiance. The actual output of the PV module is a function of orientation, total irradiance, spectral irradiance, wind speed, air temperature, soiling, and system losses.

I-V Curve of a PV Cell

I-V curve of the PV cell can be measured in direct and reverse bias. The measurements are performed in dark and illumination conditions to extend the measurement range of the I-V characteristics of the PV cells in the module [14]. If the cell operates in the forward bias region of the I-V curve, the cell generates voltage and power. If the cell operates in the reverse bias region of the I-V curve, its voltage reduces and also dissipates power [8]. The cell in reverse bias mode dissipates power in form of heat and therefore the cell temperature increases drastically. The main causes of reverse bias mode operation of the PV cell are shading, mismatch effects.

The figure 4.10 below indicates the I-V characteristics in dark conditions in reverse and direct bias conditions. There are high power dissipations in the reverse characteristics of the PV cell and the slope of reverse curves varies. Some reverse curves have flat slope (voltage limited cells) and others have steep slope (current limited cells).

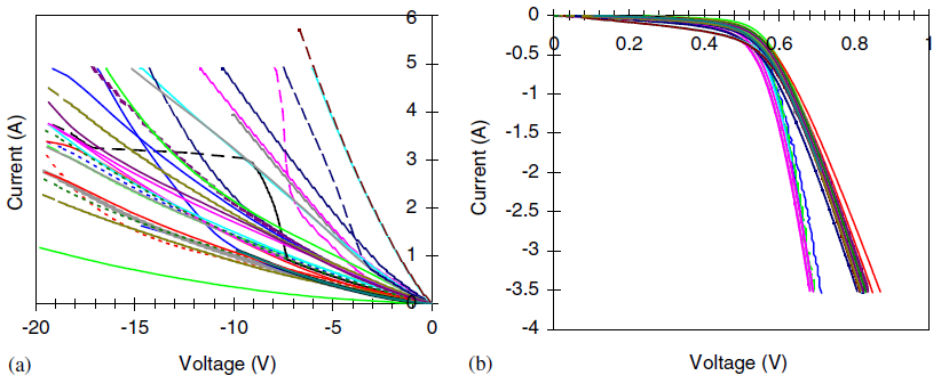

Fig. 4.10. I-V characteristics of the PV cells tested in dark conditions in reverse bias (a) and direct bias (b). T=22 ^{o}C [14]

The figure 4.11 below shows the I-V characteristics of the PV cells in a module under illumination in reverse and direct bias conditions. The graphs are for characterisation under illumination when the PV cells are tested outdoors in a cold, sunny day with stable meteorological conditions [14].

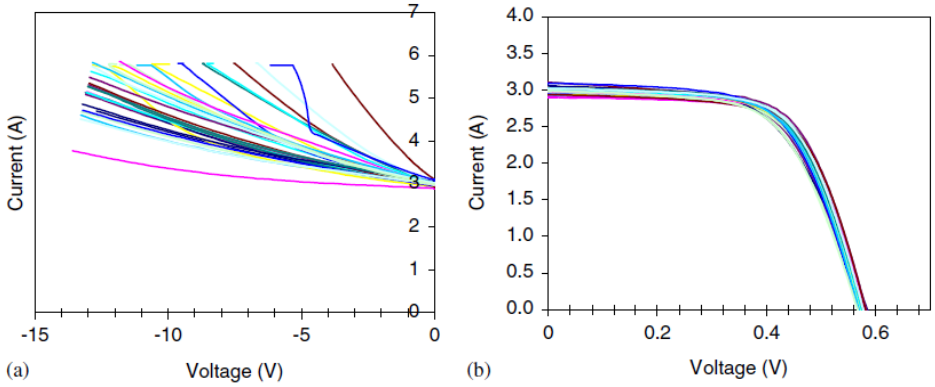

Fig. 4.11. I-V characteristics of PV cell under illumination in reverse bias (a) and forward bias (b). G=1000 W/m2, T=30 ^{o}C [14]

The shape of the cell characteristic in the reverse bias conditions is similar in darkness and illumination. PV cells with high slope in reverse bias dark conditions behave in a similar way as under illumination and also the cells with flat slope in dark conditions behave in a similar way as in under illumination.

I-V Curve of a PV Module

The characterization of I-V curves, power-voltage curves and the maximum power point tracking (MPPT) are necessary for analysing the performance of a PV cell, module or array driven loads [11].

In a string of series-connected PV cells, the resultant operating voltage is the sum of the voltages of the individual cells and the current passing through each cell is the same as the current in the external load circuit [8]. When the module contains parallel strings of series-connected cells, the voltage through each string is constant and the current in the external load circuit is sum of the currents in the strings.

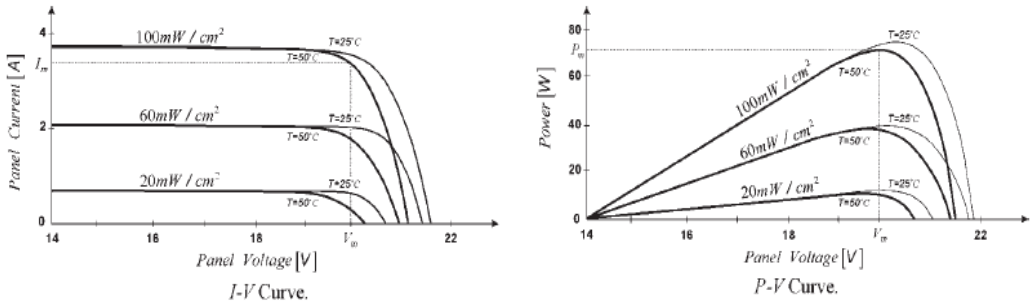

Fig. 4.12. Characteristic curves of a PV module [11]

The figure 4.12 above shows the characteristic curves of the PV module and the curves indicate the short-circuit current (I_{SC}), open-circuit voltage (V_{OC}) and the maximum power (P_m). On each point of the I-V curve, the product of current and voltage is the output power for that operating condition.

Main electrical parameters

The main electrical parameters considered in the electrical characterization of PV modules are short circuit current (I_{sc}), open circuit voltage (V_{oc}), current at maximum power (I_{mp}), voltage at maximum power (V_{mp}) and maximum power ($P_{m).}$

The experimental measurement of the I-V characteristics provides information on the actual electrical parameters of the PV module [11]. It also provides reliable knowledge on the design, installation and maintenance of PV systems. In large PV systems connected to the grid network, the measure of the I-V curves provides information on the real power installed and helps in detecting the possible damage in any string of the PV array.

Influence of external factors: irradiance, temperature, spectral irradiance

The shape of the I-V characteristics of the PV cells is generally influenced by material properties of the cell and the incident solar irradiance on the PV cell. Material parameters that affect the series and shunt resistance of the PV cell tend to alter the shape and fill factor of the I-V curve. The local irradiance conditions greatly determine the energy output of the PV systems [9]. The higher the irradiance the higher the energy output of the PV modules.

Measurements at Standard Test Conditions (STC)

The Standard Test Conditions (STC) are the irradiance of 1000 W/m^2, AM 1.5 and cell temperature of 25^{o}C. The standard procedure for determination of the electrical performance of module at STC is described in standard IEC 60904 [9]. The STC measurements are usually done by the PV manufacturers and the results included in the technical data sheet.

Measurements in real operating conditions.

These are measurements taken in real conditions of work. The irradiance and temperature are always varying in real operating conditions. When the irradiance increases, the module temperature also increases. In these conditions, when the irradiance is 1000 W/m^2, the module temperature typically operates at 40-60 ^{o}C. The nominal operating cell temperature (NOCT) is used to give a more realistic estimate of power in the field on a sunny day at solar noon. The NOCT of a module is a fixed temperature that the module would operate if exposed to nominal thermal environmental conditions (20 ^{o}C air temperature, 800 W/m^2 total irradiance and wind speed of 1 m/s).

Correction of I-V curves to STC

I-V curves obtained under the real operating conditions should be corrected to Standard test conditions (STC) using well defined procedures [12]. This is done by the correcting the characteristic curve to a module temperature 25 ^{o}C and irradiance to 1000 W/m^2. The correction coefficients are provided by the PV manufacturers. The maximum power (P_M) of the PV module can be corrected to maximum power at STC (P^*_M) using the following equation [12];

$$P^*_M = P_M . \frac{G^*}{G} . \frac{1}{[1+\gamma.(T_C - T^*_C)]} \quad (3)$$

Where;

P_M, G and T_C are maximum power, irradiance and module temperature respectively at real operating conditions.

P^*_M, G^* and T^*_C are maximum power, irradiance and module temperature respectively at STC.

γ is the power temperature coefficient provided by the PV module manufacturer.

4.4 Building Integrated Photovoltaics (BIPV)

Description and characteristics
BIPV are photovoltaic materials which are used to replace conventional building materials in parts of the building envelope for example roofs, skylights or facades [7]. The BIPV can be used for construction purposes and electricity production. This technology could be economically friendly since the initial cost can be offset by reduction of the normal construction cost of building materials and labour. BIPV is close to being capable of competing with grid electricity in certain peak demand niche markets [18].
BIPV can provide insulation over the roof of a building during summer by absorbing a large quantity of heat while also producing electricity [17].

Fig. 4.13. BIPV with photovoltaics combined with the roof [7]

Types of building integration applications
BIPV can be applied on the roofings and facades of the building. Thin film technologies are quite suitable to façade applications because of their visual appearance. The maximisation of electricity production in a building depends on the inclination of the PV modules, direction of the PV Installation and the installation distance to module length ratio (D/L).
BIPV system should have the properties of a standard roof such as water tightness, drainage and insulation [18].
The application of photovoltaics in urban areas such as BIPV requires the following stages in the development process; Setting the stage, implementation and operation. The setting stage involves the impact of renewable energy planning policy in urban areas, implementation has details of design to construction and operation involves the real success of the project [22].

Special PV modules designs for BIPV
There are many mounting systems of photovoltaics in buildings but few of them are flexible. The existing mounting systems generally require attached intermediaries and bolts for joining and fastening. In the figure 4.14 below, the photovoltaic components are fixed by the holding down plates of aluminium alloy. The plates are then fastened by bolts to the

substructures. The disadvantage of such mounting method is that it only applies to the frame-exposed BIPV systems and it cannot be installed fast due to complex wiring and numerous bolt connections.

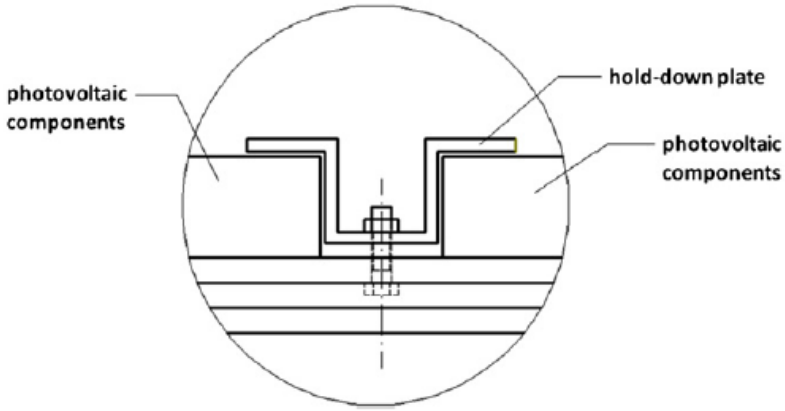

Fig. 4.14. Sketch of phovoltaic installation with a middle-pressure plate [7]

There are other ways of making the maintenance and replacement of the photovoltaic components easy and rapid e.g novel structural design. The novel structure allows easy replacement and maintenance of the photovoltaic modules. It consists of the photovoltaic cell components and a steel support system. The figure 4.15 below indicates photovoltaic cell modules, two upper-spring connection models and two under-fixed connection models closely integrated with the buildings through a steel support system. The upper-spring connection model is comprised of two springs and a sliding block in which the anode-cathode connections are at the end. One end of the spring is fixed on the sliding block and the other end is built on the U-bracket which is welded on the photovoltaic panels.

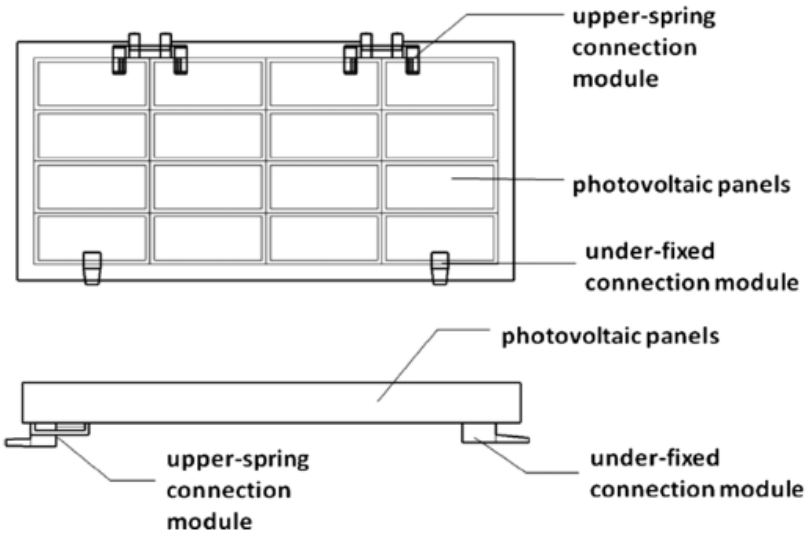

Fig. 4.15. Photovoltaic components

The steel support system consists of longitudinal beams and horizontal beams.

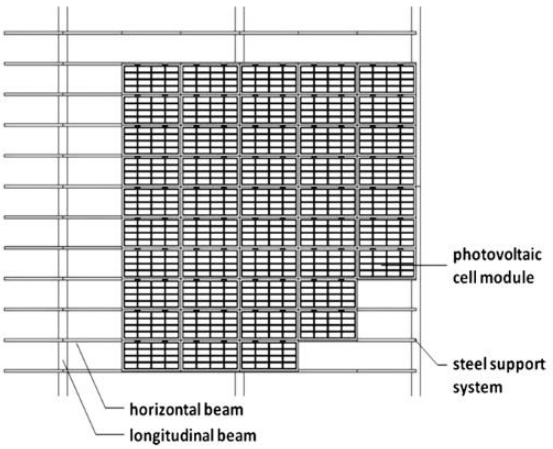

Fig. 4.16. Photovoltaic component design [7]

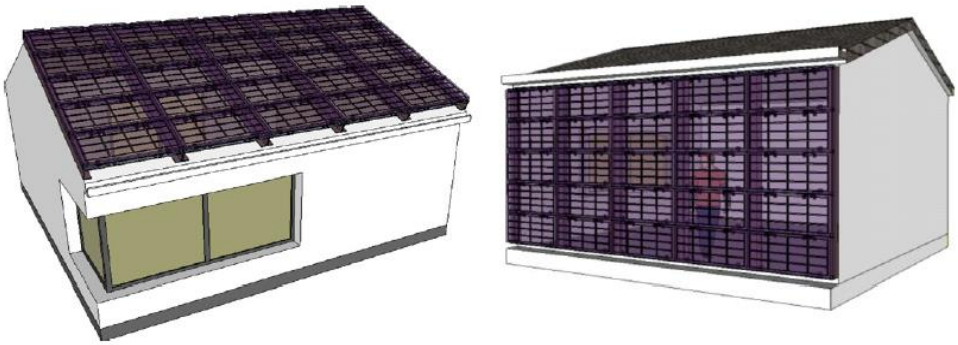

Fig. 4.17. Architectural pictures of a photovoltaic roof and photovoltaic Wall

Special operating conditions of PV modules in buildings

The factors that influence the operation of PV modules in buildings include; geographical location, solar radiation and load requirements [18]. The rating of all the loads in the building should be considered in the design of BIPV system for proper design of the PV system. The different conditions that affect the PV modules include shadows, mismatch effects, irradiance conditions, temperature and array configuration [20]. The PV modules make

shadows to other modules in the course of the day especially for inclined roofs. The irradiance and ambient temperature continuously change throughout the day. Clouds prevent the sun's radiation from reaching the PV modules and therefore, maximum PV power production occurs during clear sky conditions.

4.5 Types of shadings in BIPV

The performance of the BIPV system can be greatly affected by the kinds of shadows subjected to the system. The types of shadows in BIPV include: adjacent structures, trees [3]. The partial shading deteriorates the performance of the BIPV system. There is no electricity production when the modules are completely shaded and thus, the buildings should be constructed in a way that the roofs face the South in the Northern hemisphere and North in the Southern hemisphere. There should also be enough space between the buildings to avoid the buildings from shading other buildings in the course of the day.

4.6 The effect of shading on a PV cell

The shading may cause reduction in the power output of the PV cell because the photoelectric effect is reduced by shading. When the PV cell is fully shaded, the power production in the cell is zero and dissipates power from other cells in the series string which may cause the hot-spot phenomena to occur.

A hot-spot is a localised region in a PV cell whose operating temperature is very high when compared to the surroundings [10]. It occurs when the PV cell generates less current than the rest of the cells connected in series as a result of partial shading, cell damage, mismatch or interconnection failure. The defected cell operates in a reverse bias mode and dissipates power in form of heat.

The PV cell can be protected from hot-spots by connecting a bypass diode in parallel with the group of cells (forexample18 to 20 cells for crystalline silicon modules). Hot-spots have a potential risk of causing irreversible damage to the PV modules such as Tedlar delamination, glass breakage, loss of electrical insulation or even fire. The PV modules should be subjected to the hot-spot endurance tests to be protected against hot-spot effects.

I-V curves of a PV cell under shading
I-V curves of the PV cells operate in the reverse bias mode when shaded. Shading of the PV cells results into power dissipation instead of power generation. Bypass diodes are necessary in the PV module to enable power dissipation in only the shaded cells in the module without interrupting power generation in the unshaded cells.

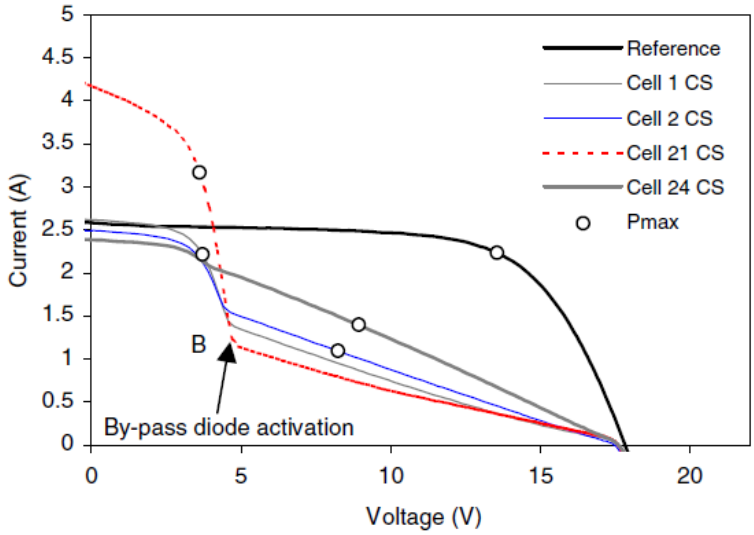

Fig. 4.18. Comparison of I-V characteristics of the test module under no shading and shading of some cells [14]

I-V characteristics of the shaded cells in the module depend on the position of the diodes in the module. The bypass diode is activated when the shaded cells are connected to the diode. The figure 4.18 above shows the I-V characteristics of the PV module under shading and the point at which diode activation takes place. The deformation of the module I-V curve increases with the amount of shading for the same PV cell shaded and maximum power point voltage is reduced to lower values.

Classification of PV cells according to their reverse I-V curve

The knowledge about the operational behaviour of the PV cells in reverse-bias conditions is very necessary to predict the hot-spot phenomena. The maximum cell temperatures depend on the shape of the I-V curve in reverse polarisation [13]. I-V characteristics in reverse polarisation of the PV cells from the same manufacturer could have variations for example they could be very flat I-V curves (voltage-limited cells), very steep I-V curves (current-limited cells) or intermediate situations [13].

4.7 Electrical and thermal effects of partial shading on a PV module

Influence of different types of shading
The different types of shading on a PV module may have an effect on the maximum power point. Shading displaces the maximum power point voltage to lower values and this may affect the systems with inverters for maximum power point tracking by increasing the power losses [15].

Influence of the type of shaded cell
Partial shading influences the reverse characteristics of the PV cell and shading all the cells in the module makes it possible to determine current limited and voltage limited cells [16]. Cells with high leakage currents experience increase in the temperature during shading conditions.

The influence of the reverse I-V characteristics of the shaded cell is more pronounced in the zone between the point at which the short circuit current (I_{sc}) of the shaded cell is surpassed and the point of bypass diode activation [15]. PV cells with high shunt conductance have less effect on the deformation of the I-V characteristics. The increase in the number of shaded cells in the same string may not have an effect on the maximum power point and when shaded cells are placed in different strings, power losses increase [15].

The effect of bypass diodes
The bypass diodes are connected in parallel to the series string of PV cells and one bypass diode can be connected to 16, 18, 20, 24 or 36 cells in a series string [16]. The activation of the bypass diode depends on the leakage current of the shaded cell and the degree of shading [13]. The higher shading fractions on the same module and configuration cause earlier activation of the bypass diode and higher current flows through the diode which results into higher power dissipation from the PV module. Considering the same shading fraction, the irradiance at which the bypass diode switches to conduction is higher when the cells with higher leakage currents are shaded. When a cell in a series string is shaded, some current flows through the cell if it has high leakage current (high slope of the reverse I-V curve) and for a cell with a flat reverse I-V curve, all the current flows through the bypass diode resulting into high power dissipation in the junction box.

I-V characteristics of the PV module are deformed by the increase in the number of cells protected by the by-pass diode and this may result in the reduction of maximum power [15].
The presence of the bypass diodes in the module causes multiple steps in the I-V characteristics and new local peaks in the P-V characteristics exist [20]. The manufacturers put bypass diodes in the modules to derive the current from the cells when voltage becomes negative and to prevent hot spot phenomena [21].

Temperature measurements and IR thermographs
The measurement of module temperatures is very necessary in determining the operational behaviour of the PV modules under different temperatures. The module temperatures can be measured using the Infra-red (IR) thermography. IR thermography is a useful tool for studying the temperature distribution of photovoltaic cell surfaces [13]. It is used to study the surface temperatures in PV modules and rapid testing of other PV system components.

The IR images complement the results of the electrical characterisation and cells in a module with high dispersion in the reverse I-V characteristics and higher leakage currents [I_L] tend to have high temperatures [16].

The influence of the irradiance and the ambient temperature

The irradiance and the ambient temperature affect the PV power production. The weather conditions (irradiance, ambient temperature) always vary which cause the variation of PV power production. The PV modules should work with the irradiance above 800 W/m^2 to increase electricity production. The PV module temperature increases with increase in the irradiance and this reduces the electricity production. The magnitude of the electrical parameters of the PV modules depends on the temperatures coefficients (alpha, beta and gamma).

5. METHODOLOGY

The PV modules of different technologies were subjected to different shadow patterns to determine the electrical and thermal characterization under shading. The measurements were carried out in outdoor conditions. The measurements were carried out to the 9 different modules which include; Cadmium Telluride (CdTe), Copper Indium Selenide (CIS), amorphous silicon heterojunction, amorphous silicon simple junction, amorphous silicon triple junction, mono-crystalline silicon (Kyocera), mono-crystalline silicon (Suntech), mono-crystalline silicon back contacts and multi-crystalline silicon.

For the study of the effects of the different shadow patterns, the I-V curve of each module technology was measured. In order to correct the measured I-V curves to the same testing conditions, the IEC 60904-1 standard was considered, in which it is necessary to know the values of alfa, internal series resistance (R_s) and curve correction factor (k). All the parameters were found from the technical data sheets except R_s and k which were calculated using the IEC 60904-1 standard.

The experiment was carried out at constant module temperature and different irradiances to determine R_s values for each module. To determine k values for each module, the experiment was carried out at constant irradiance and varying module temperatures.

5.1 Electrical and thermal measurements

Purpose

The solar modules were tested in the outdoor conditions for the electrical and thermal characterisation. The current, voltage and module temperatures were measured.

The electrical measurements were taken to determine current-voltage (I-V) relationship during the constant irradiance, constant module temperature and shading conditions. The current-voltage (I-V) relationship was determined and the I-V curves were plotted. The module temperatures were measured to determine the thermal behaviour of PV modules during shading conditions.

Apparatus

- PV modules

- Thermograph camera for measuring and recording the module temperatures
- Peak Power measuring device and I-V curve tracer (PVPM 1000CX)
- Support structure for the module
- Opaque covers to provide different shadow patterns on the module
- Wiring system to connect the components.

Procedure

The following experiments were done on the PV modules: constant irradiance, constant module temperature and shading effects,

- The irradiance was kept constant (above 800 W/m^2) and the module temperatures were increasing. The data was collected by the Peak power measuring device and I-V curve tracer. The model of the machine is PVCM 1000CX.
- The module temperature was maintained constant and the irradiance varied from around 600-1000 W/m^2
- Different shadow patterns were applied to the solar modules and the PVCM 1000X recorded the electrical measurements. The thermograph camera was used to measure and record the module temperatures.

5.2 Temperature and irradiance corrections to measured I-V characteristics

The measured I-V characteristics were corrected to the same testing conditions by employing the following equations of the IEC 60904-1 standard;

$$I_2 = I_1 + I_{SC}\left(\frac{G_2}{G_1} - 1\right) + \alpha(T_2 - T_1) \quad (4)$$

$$V_2 = V_1 - R_S(I_2 - I_1) - kI_2(T_2 - T_1) + \beta(T_2 - T_1) \quad (5)$$

Where;

I_1, V_1: Coordinates of points on the measured characteristics

I_2, V_2: Coordinates of the corresponding points on the corrected characteristics

G_1: Irradiance measured with the reference device

G_2: Irradiance measured at the desired irradiance

T_1: Measured temperature of the PV module

T_2: Desired temperature of the PV module

I_{SC}: Measured short circuit current of the test specimen at G_1 and T_1

α, β: Current and voltage temperature coefficients of the PV module in the target irradiance for correction and within the temperature range of interest

R_s: Internal series resistance of the PV module

k : Curve correction factor

The current and voltage temperature coefficients were given in the PV module data sheet.

5.3 Determination of the internal series resistance, R_s

The determination of R_s was done following the IEC 60891 standard. The experiment was carried out at constant module temperature and different irradiances. During the I-V measurements, the module temperatures were stable within $\pm 2^o C$. The current-voltage curves were plotted and analysed. The plotted I-V curves would appear as in the figure 1a.

Correction procedure

- I_{SC1} was taken to be the short-circuit current of the I-V characteristics recorded at the highest irradiance G_1. I-V curves recorded at lower irradiances (G_2…..G_N) were translated to the I-V curve of the highest irradiance G_1 when R_S=0Ω. The maximum output power values were determined from the I-V measurements.

- The corrected I-V curves were plotted and would appear as in figure 5.1b

- The series resistance R_S was changed in the steps of 10 mΩ in the positive or negative direction. The optimal value of R_s was obtained when the deviation of the maximum output power values of the transposed I-V characteristics was within $\pm 0.5\%$. The optimal graph would appear as in figure 5.1c.

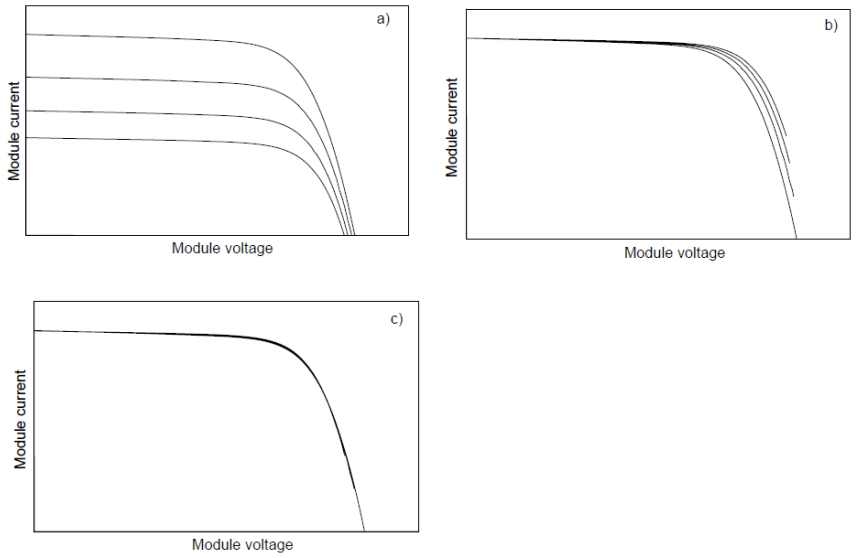

a) Measured I-V characteristics at different irradiances and constant temperature

b) Corrected I-V characteristics at R_S = 0 Ω

c) Corrected I-V characteristics at R_S = optimal

Fig. 5.1. Determination of internal series resistance, R_s

5.4 Determination of the curve correction factor k

The determination of k was done following the IEC 60891 standard. The experiment was carried out at a constant irradiance and different module temperatures. During the I-V measurements, the irradiances were stable within $\pm 1\%$. The current-voltage curves were plotted and analysed. The plotted I-V curves would appear as in the figure 5.2a. The temperature coefficients α and β were already provided in the PV module manufacturer data sheet.

Procedure

- The current-voltage characteristics of the PV module at constant irradiance and varying temperatures were recorded. The maximum output power values were determined and the I-V characteristics were as shown in figure 5.2a.

- T_1 was taken to be the lowest module temperature and the I-V curve plotted. The higher module temperatures (T_1……T_N) were translated to the lowest temperature I-V characteristics using k=0 Ω.

- The corrected I-V curves were plotted (see figure 5.2b)

- The curve correction factor k was varied from 0 mΩ in the steps of 1mΩ in the positive or negative direction. The optimum value of k was obtained when the deviation of maximum output power values of the transposed characteristics coincided within $\pm 0.5\%$

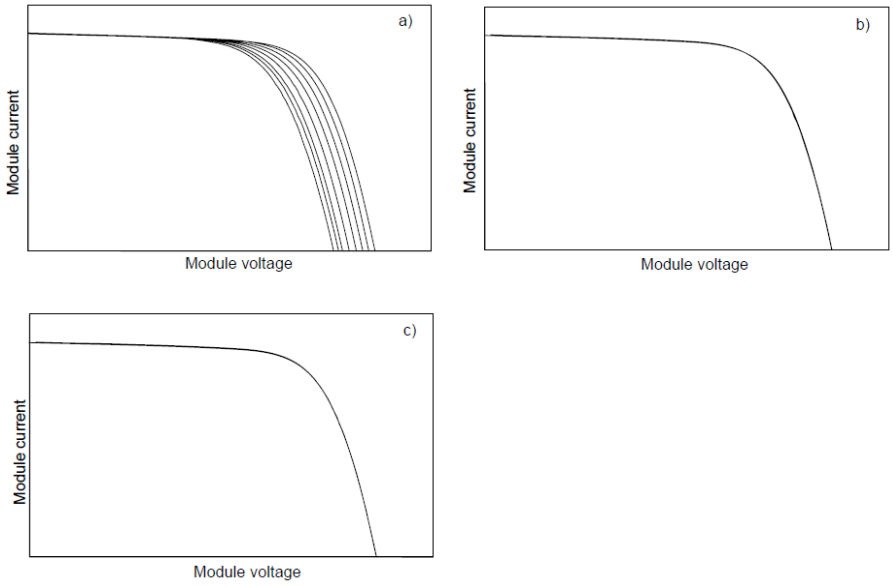

a) Measured I-V characteristics at different device temperatures.

b) Temperature corrected I-V characteristics with κ = 0 Ω/K or κ' = 0 Ω/K.

c) Corrected I-V characteristics with κ = optimal or κ' = optimal.

Fig. 5.2. Curve correction factor determination

5.5 PV modules considered in the experiments

The electrical and thermal characterisation was done on the 9 different technologies of solar modules from different manufacturers. The modules tested are indicated in the table below;

Table. 5.1. Photovoltaic modules tested

Technology	**Manufacturer**	**Model**	**Serial no.**	**No. of cells**	**No. of Bypass diodes**
CdTe	First Solar	FS-380	101012081700	154s	None
CIS	Würth	WSG0036 E80	01-100929-00781-001	134s	None
a-Si heterojunction	Sanyo HIT	240HDE4	A2FA10068	10s*6p	2
a-Si simple junction	Kaneka	GEA-060	6EA521-108101481156061X1	110s	None
a-Si triple junction	Unisolar	ES-62T		11s	1
m-Si	Kyocera	KD210GH-2PU	101JHRK533	18s*3p	1
m-Si	Suntech	STP175s_24/Ac	12210338501610700	6s*12p	2
m-Si back contacts	Sunpower	SPR_238E_WHT_D	G23P01317978	72s	3
mc-Si	Atersa	A-180P	1011002007067	6s*12p	2

Table. 5.2. PV modules characteristics from manufacturer data sheets

	A	V	W	% / ° C	% / ° C	% / ° C	°C
Technology	I_{sc}	V_{oc}	P_m	Alfa	Beta	Gamma	NOCT
CdTe	1.76	61.7	80	0.040	-0.27	-0.25	44
CIS	2.5	44	80	0.050	-0.29	-0.36	47
a-Si heterojunction	7.37	43.6	240	0.030	-0.25	-0.30	45
a-Si simple junction	1.19	92	60	0.075	-0.31	-0.23	45
a-Si triple junction	5.1	21	62	0.100	-0.00038	-0.21	46
m-Si (Kyocera)	8.58	33.2	210	0.058	-0.00036	-0.46	49
m-Si (Suntech)	5.2	44.2	175	0.017	-0.34	-0.48	45
m-Si back contacts	5.88	48.5	238	0.060	-0.00027	-0.38	46
mc-Si	5.4	44.12	180	0.080	-0.32	-0.43	48

5.6 Shadow patterns classification

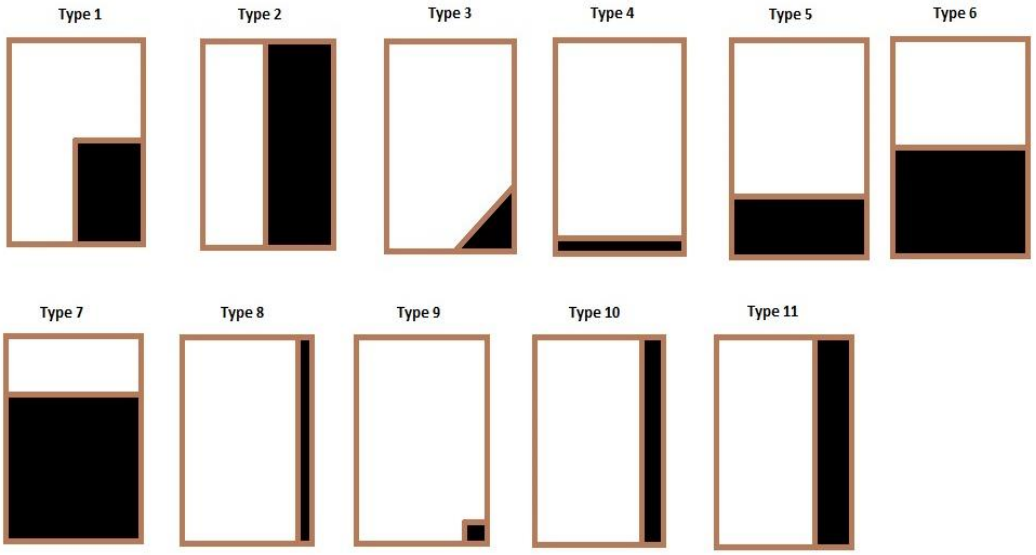

Fig. 5.3. Shadow pattern classification

Table. 5.3. Shadow pattern explanation

Shadow pattern	**Explanation**
Type 1	1/4 of module shaded
Type 2	half module shaded vertically
Type 3	part of the module vertex shaded
Type 4	one cell shaded
Type 5	Several cells shaded horizontally (less than ½ module)
Type 6	Half module shaded horizontally
Type 7	3/4 of the module shaded horizontally
Type 8	one line of cells shaded vertically
Type 9	One cell shaded on the module vertex
Type 10	2 lines shaded vertically
Type 11	1/4 of module shaded vertically

5.7 PV module experiments

Cadmium Telluride (CdTe)

The experiment was done for constant irradiance-variable module temperature and for constant module temperature-variable irradiance. The electrical characteristics were then measured. The different shadow patterns were applied on the module. The electrical and thermal properties of the module were measured. The weather conditions were; clear sky and no clouds.

The shadow patterns which were subjected to the module are; Type 1 (1/4 of module shaded), Type 4 (one cell shaded), Type 5 (10 cells shaded horizontally), Type 5 (20 cells shaded horizontally), Type 6 (Half module shaded horizontally), Type 7 (3/4 of the module shaded horizontally), Type 3 (part of the module vertex shaded), Type 2 (half module shaded vertically).

Fig. 5.4. Cadmium Telluride module

Copper indium selenide (CIS)

The module was subjected to constant irradiance-variable module temperature and constant temperature-variable irradiance. The constant irradiance considered was around 880 W/m^2 and constant module temperature was around 51.7 ^{o}C. The different shadow patterns were applied to the module; Type 2 (half module shaded vertically), Type 6 (half module shaded horizontally), Type 10 (2 lines shaded vertically), Type 11 (1/4 of module shaded vertically), Type 1 (1/4 of module shaded), Type 3 (small edge of module shaded).

(a)

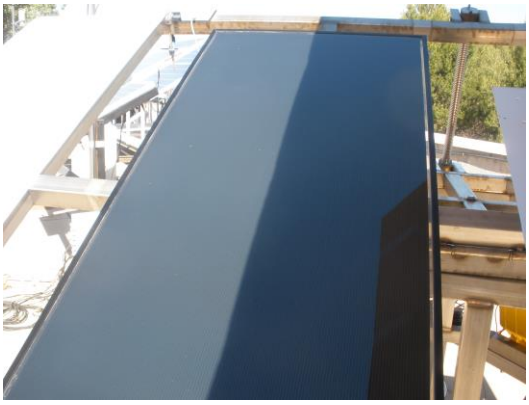

(b)

Fig. 5.5. Copper indium selenide module *for (a) Unshaded and (b) type 2 shadow*

Amorphous silicon (a-Si) heterojunction

The constant irradiance-variable module temperature and constant module temperature-variable irradiance were applied to the a-Si heterojunction module. The constant irradiance considered was around 880 W/m^2 and constant module temperature was around 51.4 ^{o}C.

The different shadow patterns were applied to the module; Type 2 (Half module shaded vertically), Type 6 (half module shaded horizontally), Type 1 (1/4 module shaded), Type 3 (Part of the module vertex shaded), Type 4 (one line shaded horizontally), Type 8 (One line shaded vertically), Type 9 (One cell shaded on the module vertex). The electrical and thermal characteristics of the module were measured and recorded by the I-V tracer and the thermograph camera respectively. The experiments were carried out in good weather conditions (clear sky and no clouds).

Fig. 5.6. Amorphous silicon heterojunction module

Amorphous silicon (a-Si) simple junction

The module was subjected to the constant irradiance-variable module temperature and constant module temperature-variable irradiance conditions. The constant irradiance was around 804 W/m^2 and the constant module temperature was around 51.5 ^{o}C. The weather conditions were not very clear sky (thin clouds).

The following shadow patterns were applied to the module; type 1, type 2, type 3, type 6, type 8 (one line of cells shaded vertically), type 7, type 10 (2 lines of cells shaded vertically) and type 11.

Fig. 5.7. Amorphous silicon simple junction module

Amorphous silicon (a-Si) triple junction

The a-Si triple junction module was subjected to constant irradiance-variable module temperature and constant module temperature-variable irradiance. The constant irradiance was around 880 W/m^2 and the module temperature around 51.4 ^{o}C. The following shadow patterns were applied to the module: type 1, type 2, type 3, type 4 (one line shaded horizontally), type 5 (3 lines shaded horizontally), type 6 and type 7.

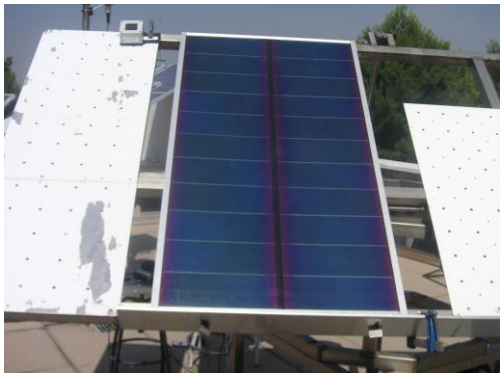

Fig. 5.8. Amorphous silicon triple junction module

Monocrystalline silicon (m-Si) -Kyocera

The module was subjected to constant irradiance-variable module temperature and constant module temperature-variable irradiance. The constant irradiance was around 860 W/m^2 and the constant module temperature was around 50.2 ^{o}C. The following shadow patterns were applied to the module: type 1, type 2, type 3, type 4, type 5 (3 lines shaded horizontally), type 6, type 8, type 9, type 7, type 10 (2 lines shaded vertically) and type 11.

Fig. 5.9. Monocrystalline silicon module (Kyocera)

Monocrystalline silicon (m-Si)-Suntech

The module was subjected to constant irradiance-variable module temperature and constant module temperature-variable irradiance. The constant irradiance was around 824 W/m^2 and the constant module temperature was around 55.1 ^{o}C. The following shadow patterns were applied to the module: type 1, type 2, type 3, type 4, type 5 (4 lines shaded horizontally), type 6, type 8, type 9, type 7, type 10 (2 lines shaded vertically) and type 11.

Fig. 5.10. Monocrystalline silicon module (Suntech)

Monocrystalline silicon (m-Si) back contacts

The constant irradiance-variable module temperature and constant module temperature-variable irradiance were applied to the m-Si back contacts module. The experiments were carried out in moderate weather conditions (clear sky, no clouds and a little windy).

The constant irradiance considered was around 880 W/m^2 and constant module temperature was around 51.5 ^{o}C. The different shadow patterns were applied to the module; type 1, type 2, type 4, Type 6, Type 8, Type 3, Type 9 (small edge of the module shaded) and type 10 (2 lines shaded vertically).

The electrical and thermal characteristics of the module were measured and recorded by the I-V tracer and the thermograph camera respectively.

(a)

(b)

Fig. 5.11. Monocrystalline silicon back contacts with (a) module (b) Experimental set up

Multi-crystalline silicon

The constant irradiance-variable module temperature and constant module temperature-variable irradiance were applied to the module. The constant irradiance was around 830 W/m^2 and constant module temperature was around 51.4 ^{o}C. The weather conditions were clear sky with few clouds.

The following shadow patterns were applied to the module; type 1, type 2, type 3, type 4, type 5 (4 lines shaded horizontally), type 6, type 8, type 9, type 7, type 10 (2 lines shaded vertically) and type 11.

Fig. 5.12. Multi-crystalline silicon module

6. RESULTS AND DISCUSSIONS

This chapter contains the results and discussions of the electrical and thermal characteristics of the PV module technologies under shading. R_s, k, alpha and beta values were used to correct the I-V characteristics to the same conditions. Each module technology was subjected to different shadow patterns. The electrical and thermal results for each module technology under different shadow patterns were analysed.

The different PV module technologies under the same shading pattern were also compared to determine their behaviour under the same shading conditions. The maximum power was corrected to standard test conditions (STC) to compare the module technologies under the same shading conditions. The unshaded module was taken as a reference and variation of maximum power at STC for all shadow patterns from the reference was analysed. The results indicate the PV module technologies behave differently under the same shadow pattern.

The shadow patterns resulted into the reduction of the electrical characteristics (current, voltage and power) for each module technology. The shading also resulted into the reduction of the maximum power of each module technology and there were no hot spots in the modules.

In general, shading reduces the electrical parameters of the modules but the magnitude of the electrical parameters depends on the shadow patterns, arrangement of the cells and location of bypass diodes in the modules.

6.1 Electrical characteristics of the PV modules under shading

Cadmium Telluride (CdTe)

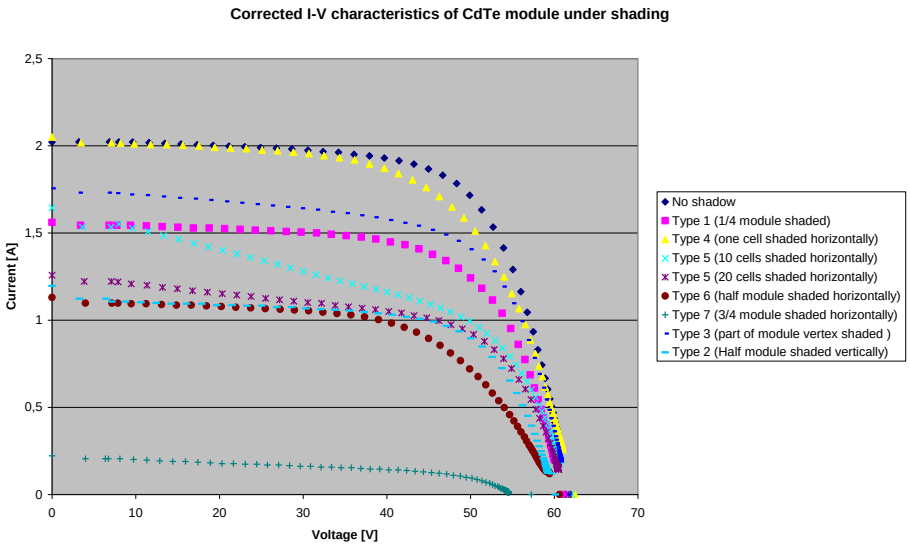

Fig. 6.1. Corrected I-V characteristics of CdTe module under shading

The cells in the CdTe module were arranged horizontally. The figure 6.1 above indicates that shading reduces the electrical parameters such as current, voltage and power. The CdTe module did not have bypass diodes because the I-V curves follow a similar trend and the curves do not have multiple steps. Type 4 shadow had the least effect on the electrical parameters and Type 7 shadow had the highest effect on the electrical characteristics of the CdTe module.

The CdTe module did not have any bypass diodes connected and this greatly affected the power production because electrical power was dissipated in form of heat due to reverse flow current. In general, shading reduces the electrical parameters of CdTe module but the magnitude of the electrical parameters depends on the shadow patterns and arrangement of the cells in the module.

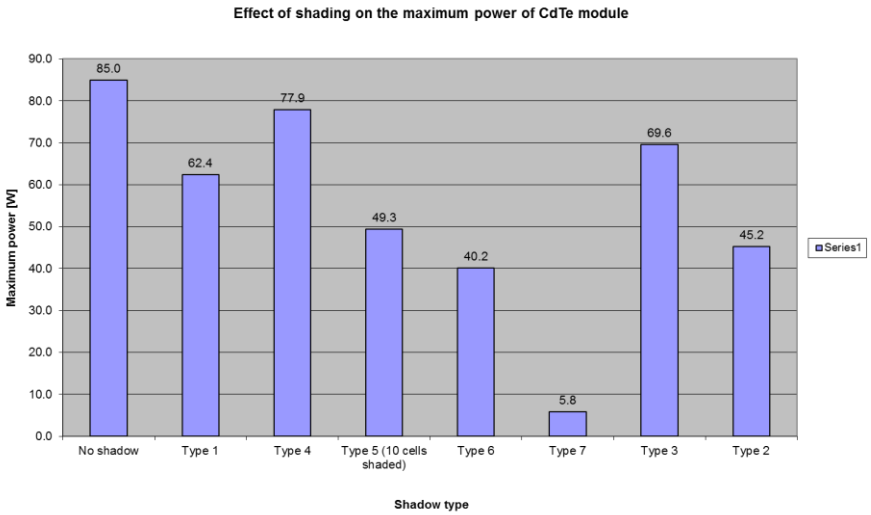

Fig. 6.2. Effect of shading on the maximum power of CdTe module

The figure 6.2 above shows the effect of shading on the maximum power of the CdTe module. The shadow that produced the highest maximum power was type 4 shadow (77.9 W) and the lowest maximum was obtained from type 7 shadow (5.8 W). The reference was the unshaded CdTe module and it had the highest maximum power (85 W). Shading reduces the maximum power of the CdTe module and magnitude of the maximum power depends on the shadow pattern and cell arrangement in the module.

Copper indium selenide (CIS)

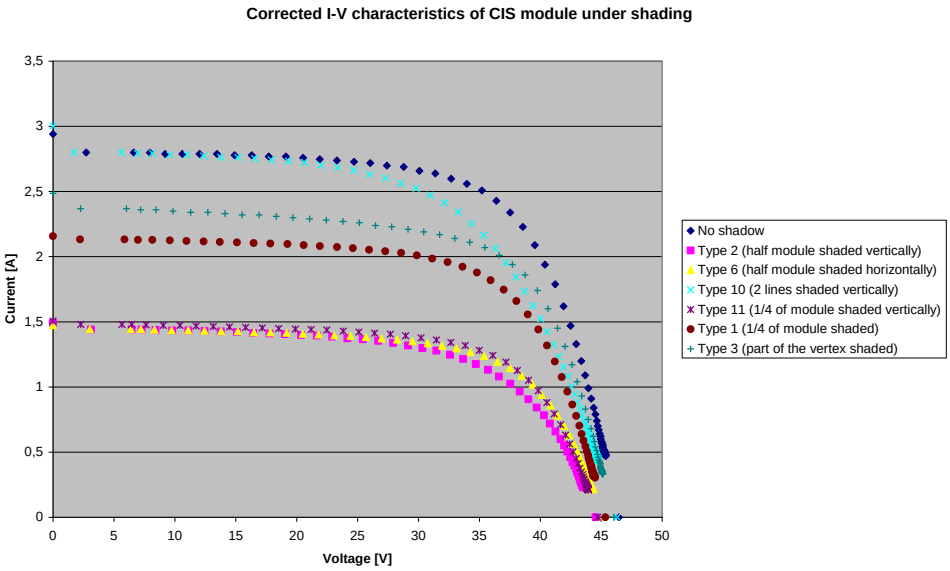

Fig. 6.3. Corrected I-V curves for CIS module under shading

The cells in the CIS module were arranged in a vertical direction. The reference (unshaded CIS module) had the highest electrical parameters such as current, voltage and maximum power as shown in the figure 6.3 above. The CIS module did not have bypass diodes since the I-V curves follow a similar trend and there are no sudden changes in the current. When there are the bypass diodes in the module, the current decrease suddenly to a lower value at a constant voltage and the power produced also reduces to a lower level.

Among the shadow patterns, type 10 produced the highest electrical parameters (short circuit current, open circuit voltage and maximum power) and type 2 produced the lowest electrical parameters. The figure 6.3 indicates that the increase in the shadow area results into the decrease in the electrical parameters of the module. The increase in the shadow area reduced the electrical power produced by the module.

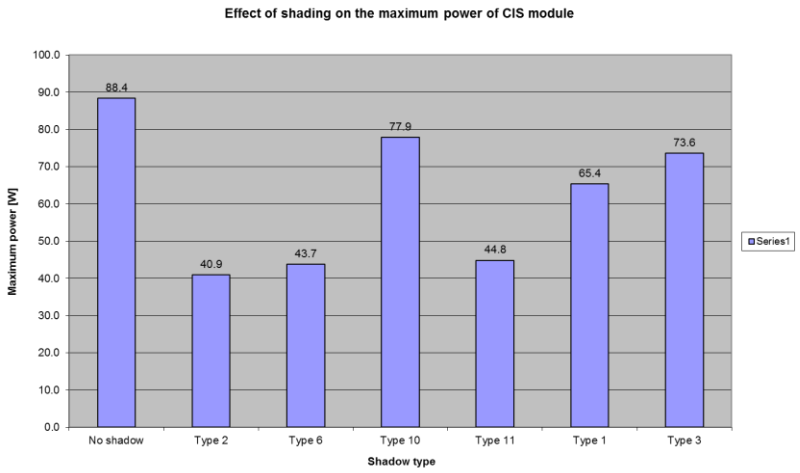

Fig. 6.4. Effect of shading on the maximum power of CIS module

The figure 6.4 above shows that the reference (no shaded module) produced the highest maximum power (88.4 W). Among the shadow patterns, type 10 produced the highest maximum power (77.9 W) and type 2 shadow produced the lowest maximum power (40.9 W). The shadow patterns on the module resulted into the reduction of the maximum power produced by the CIS module.

Amorphous silicon (a-Si) heterojunction

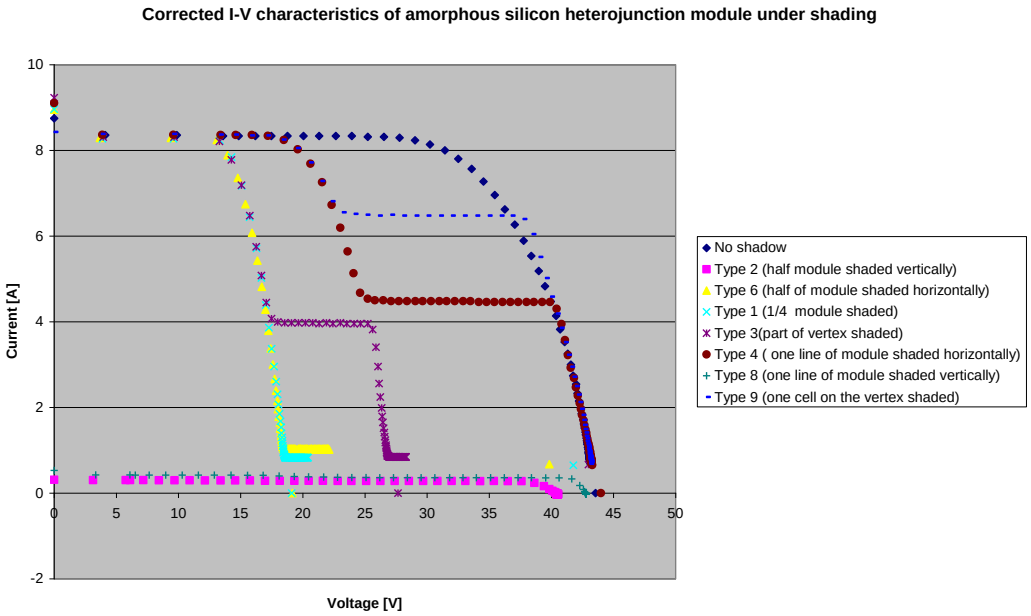

Fig. 6.5. Corrected I-V characteristics of amorphous silicon heterojunction module under shading

The figure 6.5 above indicates that the reference condition (unshaded module) had the highest electrical parameters (current, voltage and maximum power). Among the shadows, type 9 had the highest electrical parameters and type 2 had the lowest electrical parameters. The figure 6.5 also shows that the a-Si heterojunction module had 2 bypass diodes because type 3 shadow produced 2 discrete steps of current (current reduction at constant voltage and increase in voltage at constant current).

One bypass diode was activated by the following shadow patterns; type 9, type 4, type 6 and type 1.The two bypass diodes were activated by type 3. The bypass diodes were not activated by type 2 and type 8.

The magnitude of electrical characteristics produced by shading the a-Si heterojunction module depends on the shadow patterns, cells arrangement and arrangement of the bypass diodes in the module. Therefore, shading reduces the electrical characteristics to lower values compared to the unshaded module (reference).

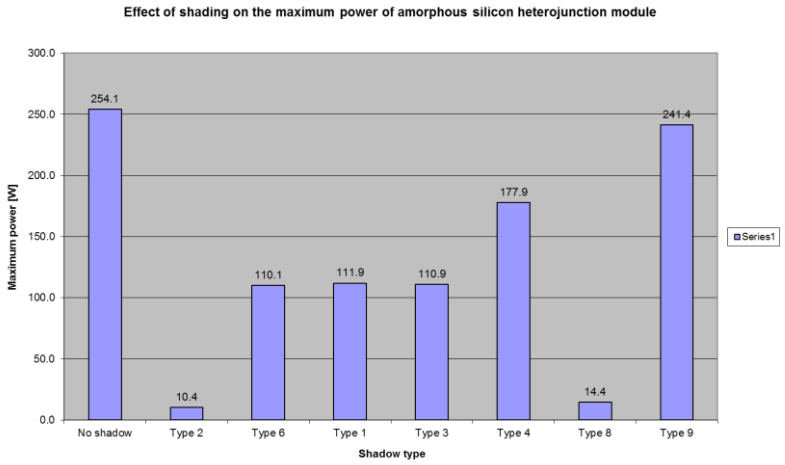

Fig. 6.6. Effect of shading on the maximum power of a-Si heterojunction module

The figure 6.6 above shows that the unshaded a-Si heterojunction module produced the highest maximum power (254.2 W) and was taken to be the reference. Considering the shadow patterns, type 9 shadow produced the highest maximum power (241.4 W) and type 2 shadow produced the lowest maximum power (10.4 W).

In general, shading reduces the maximum power of the a-Si heterojunction module but the magnitude of the maximum power depends on the shadow pattern, arrangement of cells in the module and the location of the bypass diodes.

Amorphous silicon (a-Si) simple junction

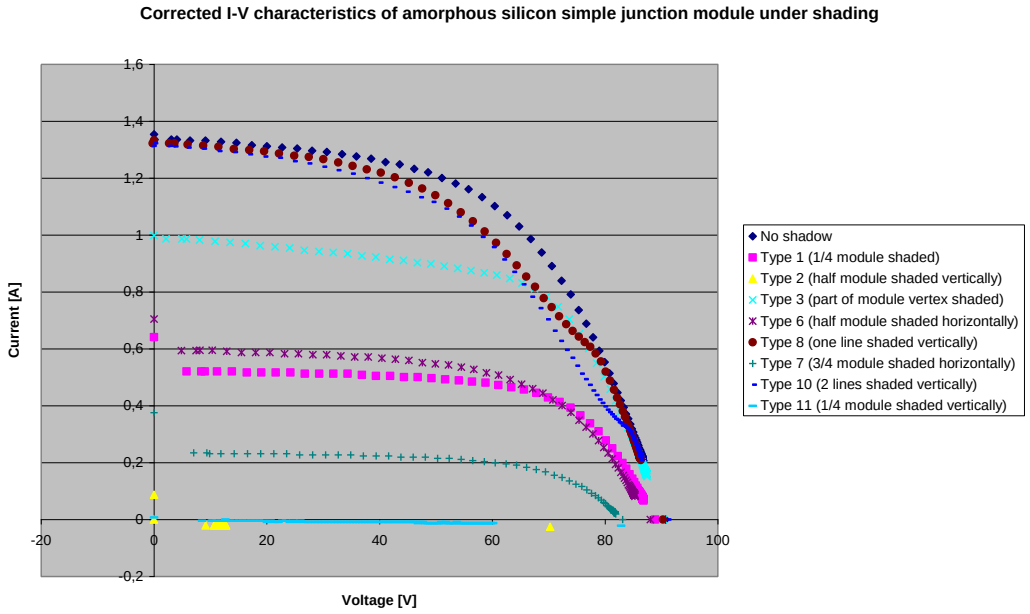

Fig. 6.7. Corrected I-V characteristics of a-Si simple junction module under shading

The cells in the a-Si simple junction module were arranged in a vertical position. There was a reduction in the module parameters (current, voltage and maximum power) due to shading as shown in the above figure 6.7. The unshaded module was taken as the reference and produced the highest electrical parameters. When the shadow patterns were compared, the type 8 produced the highest electrical parameters and type 2 produced the lowest electrical parameters.

The graph 6.7 above indicates that there were no bypass diodes in the a-Si simple junction module which caused the power losses in the module to increase. The shading of the a-Si simple junction module resulted into the decrease in the electrical power produced and therefore shading should be avoided as much as possible when the module is in operation.

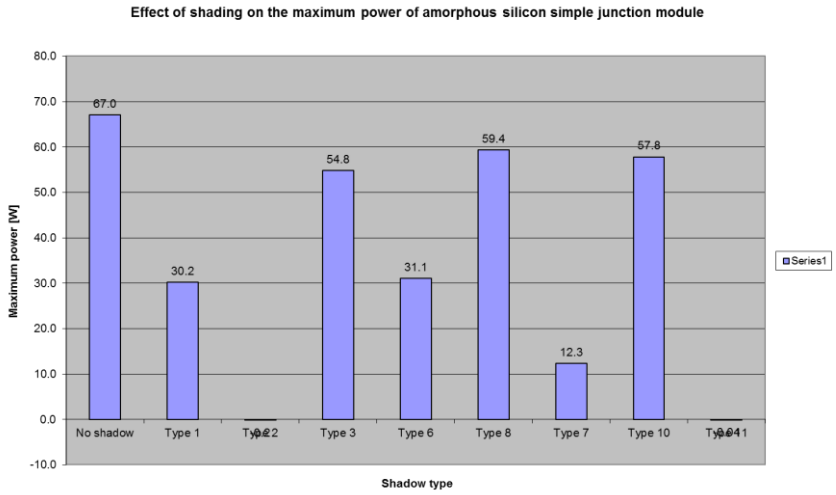

Fig. 6.8. Effect of shading on the maximum power of a-Si simple junction module

The figure 6.8 above indicates the unshaded module (reference) produced the highest maximum power (67 W). Among the shadow patterns, type 8 produced the highest maximum power (59.4 W) and type 2 dissipated power (-0.2 W). The dissipation of power by type 2 shadow (-0.2 W) and type 11 shadow (-0.04 W) may have been caused by power losses due to mismatch effects and absence of bypass diodes. Therefore, the shading of the a-Si simple junction module results into the reduction in the maximum power produced.

Amorphous silicon (a-Si) triple junction

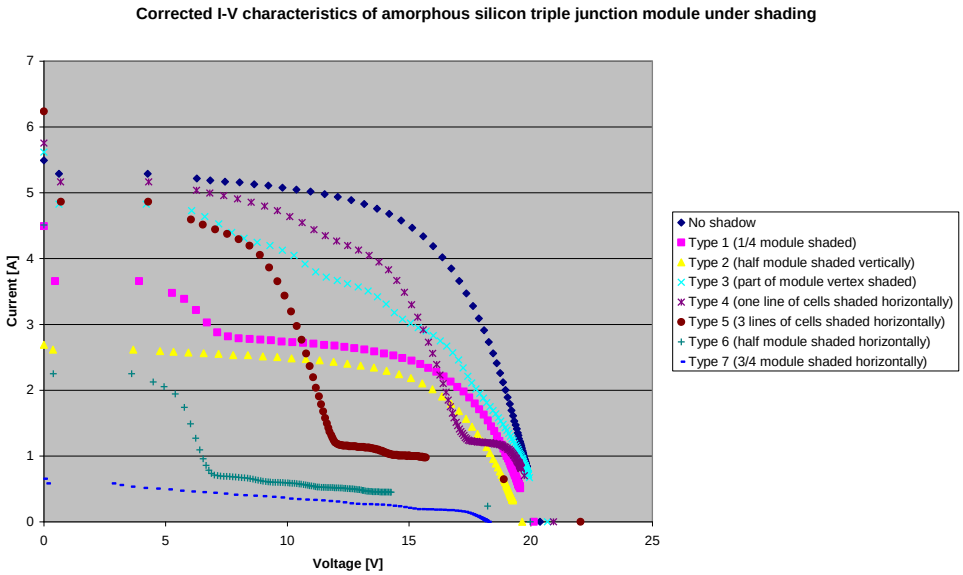

Fig. 6.9. Corrected I-V characteristics of a-Si triple junction under shading

The cells in the a-Si triple junction module were arranged in a horizontal position. The figure 6.9 above shows that shading reduces the electrical parameters (current, voltage and maximum power) of the a-Si triple junction module. The unshaded module was taken as a reference and produced the highest electrical parameters.

Considering the shadow patterns, type 4 had the highest electrical parameters and type 7 had the lowest electrical parameters. The figure 6.9 indicates that the a-Si triple junction module had the one bypass diode installed. The bypass diode was activated by the following shadow patterns; type 4, type 5, type 1 and type 6.

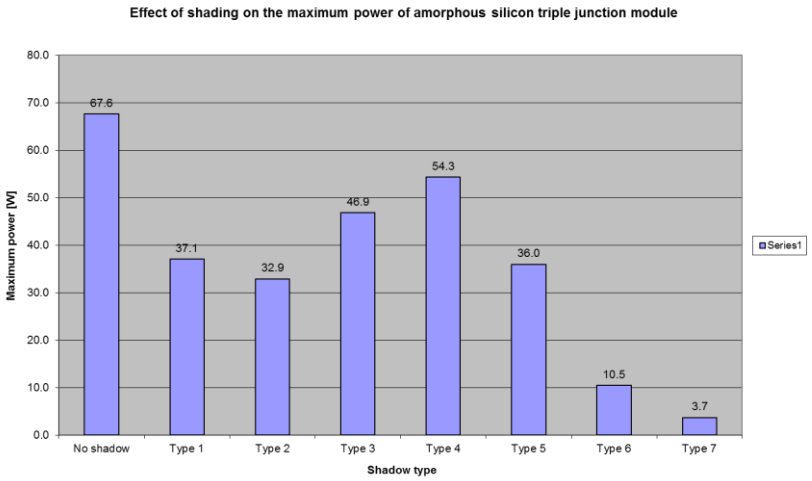

Fig. 6.10. Effect of shading on the maximum power of a-Si triple junction module

The figure 6.10 above indicates that the reference condition (unshaded module) of the a-Si triple junction module produced the highest maximum power (67.6 W). Among the shadow patterns, type 4 produced the highest maximum power (54.3 W) and type 7 produced the lowest maximum power (3.7 W).

Basing on the above results, the shading of the a-Si triple junction module decreases the electrical power production and thus, shading should always be avoided in the real operating conditions.

Monocrystalline silicon (Kyocera)

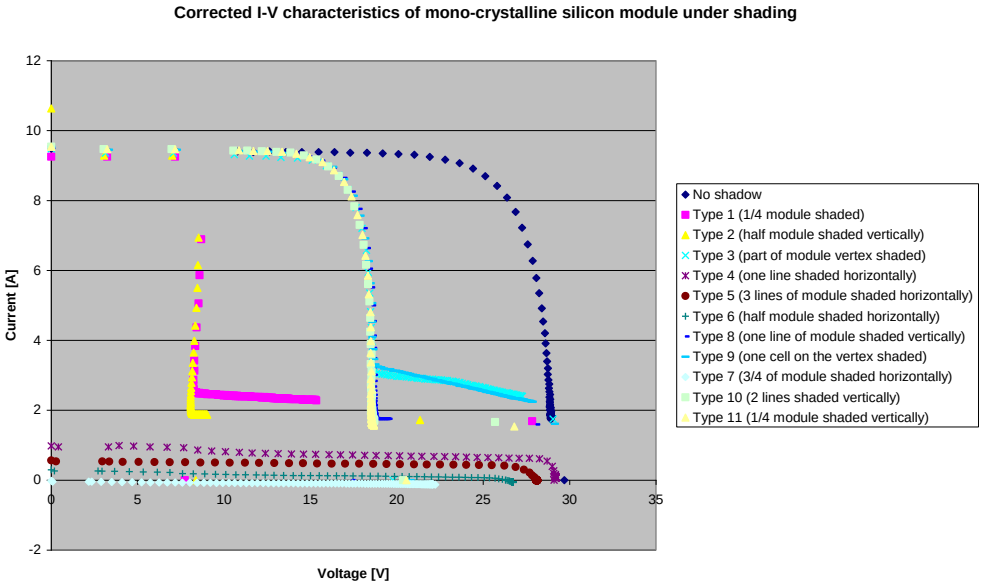

Fig. 6.11. Corrected I-V characteristics of m-Si module (Kyocera) under shading

The highest electrical characteristics (current, voltage and maximum power) were produced by the unshaded m-Si module-Kyocera (reference) as shown in the figure 6.11 above. Shading led to the reduction of the electrical characteristics of the module.

Comparing the shadow patterns, type 9 produced the highest electrical characteristics and type 7 produced the lowest electrical characteristics. The figure 6.11 shows that the m-Si had one bypass diode. The bypass diode was activated by the following shadow patterns; type 9, type 8, type 11, type 3, type 2 and type 1. The rest of the shadow patterns did not activate the diode. Basing on results of the m-Si module (Kyocera), shading decreased the electrical characteristics of the module.

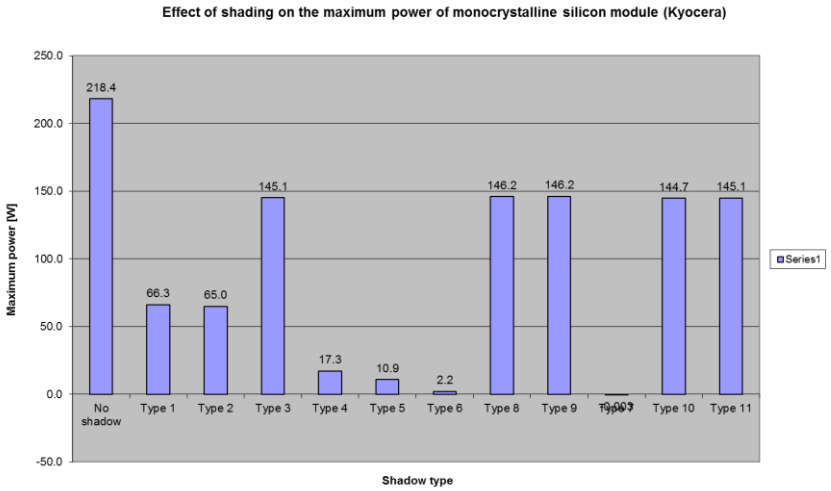

Fig. 6.12. Effect of shading on the maximum power of m-Si module (Kyocera)

The reference condition of the m-Si module-Kyocera (unshaded module) produced the highest maximum power (218.4 W). Considering the shadow patterns, type 9 shadow produced the highest maximum power (146.2 W) and type 7 shadow dissipated power instead of power production (-0.003 W). The above figure 6.12 indicates shading reduces the maximum power produced by the m-Si (Kyocera) module and should be avoided as much as possible.

Monocrystalline silicon (Suntech)

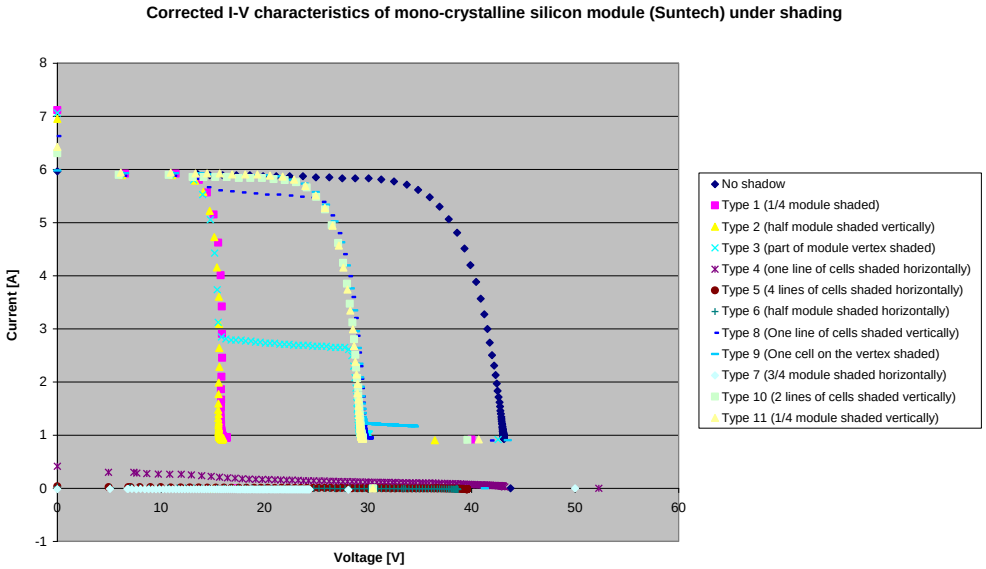

Fig. 6.13. Corrected I-V characteristics of m-Si module (Suntech) under shading

The highest electrical characteristics (current, voltage and maximum power) were produced by the unshaded m-Si module-Kyocera which was taken as reference as shown in the figure 6.13 above. Shading led to the reduction of the electrical characteristics of the module.

Comparing the shadow patterns, type 9 produced the highest electrical characteristics and type 7 produced the lowest electrical characteristics. The figure 6.13 shows that the m-Si had two bypass diodes. The two bypass diodes were activated by the following shadow patterns; type 3 and type 8. The following shadow patterns activated only one bypass diode; type 1, type 2, type 9, type 10 and type 11.

The rest of the shadow patterns did not activate the bypass diodes. Basing on results of the m-Si (Suntech) module, shading decreased the electrical characteristics of the module.

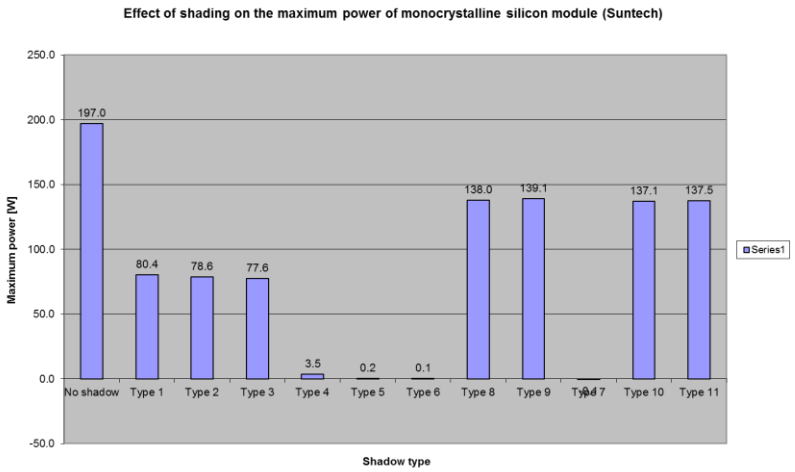

Fig. 6.14. Effect of shading on the maximum power of m-Si module (Suntech)

The reference condition of the m-Si module-Suntech (unshaded module) produced the highest maximum power (197 W). Considering the shadow patterns, type 9 shadow produced the highest maximum power (139.1 W) and type 7 shadow dissipated power instead of power production (-0.1 W).

The above figure 6.14 indicates, shading reduces the maximum power produced by the m-Si (Kyocera) module.

Mono-crystalline silicon (m-Si) back contacts

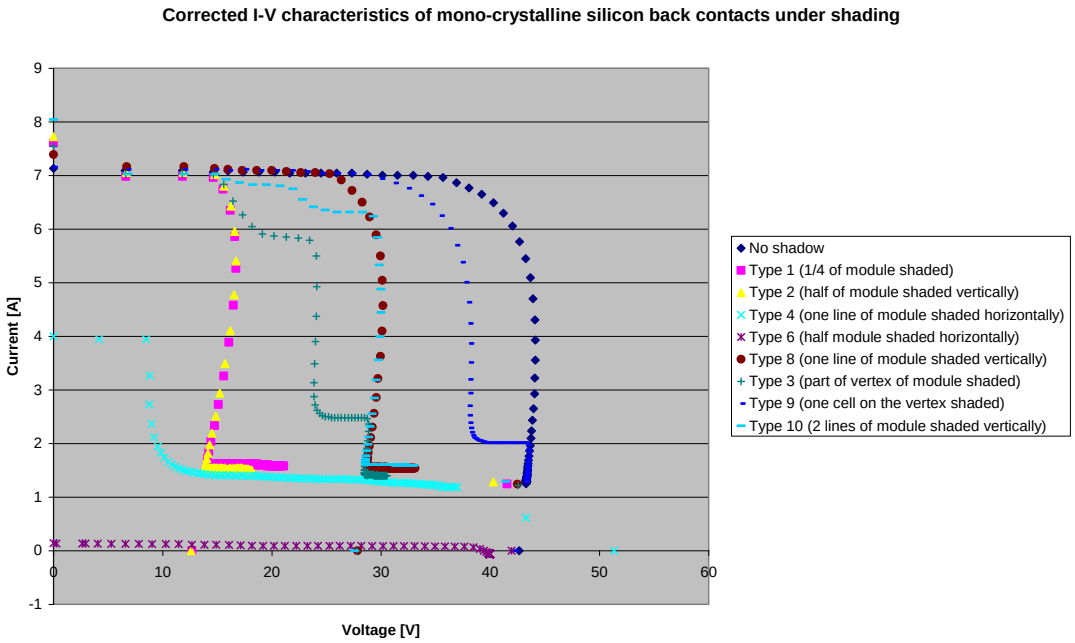

Fig. 6.15. Corrected I-V characteristics of m-Si back contacts module under shading

The unshaded module was taken as a reference and it produced the highest electrical characteristics (current, voltage and maximum power) as shown in the figure 6.15 above. Comparing the shadow patterns, type 9 produced the highest electrical characteristics and type 6 produced the lowest electrical characteristics.

The figure 6.15 above figure indicates that the m-Si back contacts module had 3 bypass diodes. Type 3 shadow activated all the 3 bypass diodes and type 10 activated 2 bypass diodes of the m-Si back contacts module. One bypass diode in the module was activated by the following shadow patterns; type 9, type 8, type 1, type 2 and type 4. Type 6 did not activate any of the bypass diodes.

The figure 6.15 above indicates that shading reduces the electrical characteristics of the m-Si back contacts module.

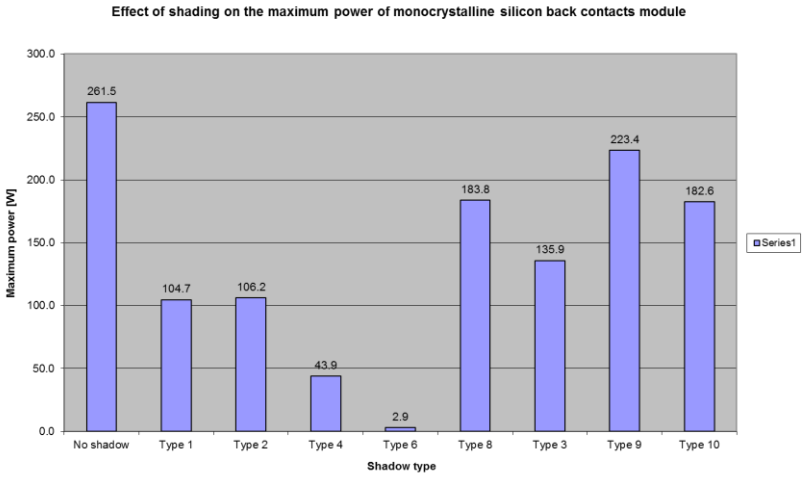

Fig. 6.16. Effect of shading on the maximum power of m-Si back contacts module

The unshaded module (reference) produced the highest maximum power (261.5 W). Considering the shadow patterns, type 9 produced the highest maximum power (223.4 W) and type 6 produced the lowest maximum power (2.9 W).

The above figure 6.16 indicates that shading reduces the maximum power of the m-Si back contacts module and should be avoided in real operating conditions.

Multicrystalline silicon (mc-Si)

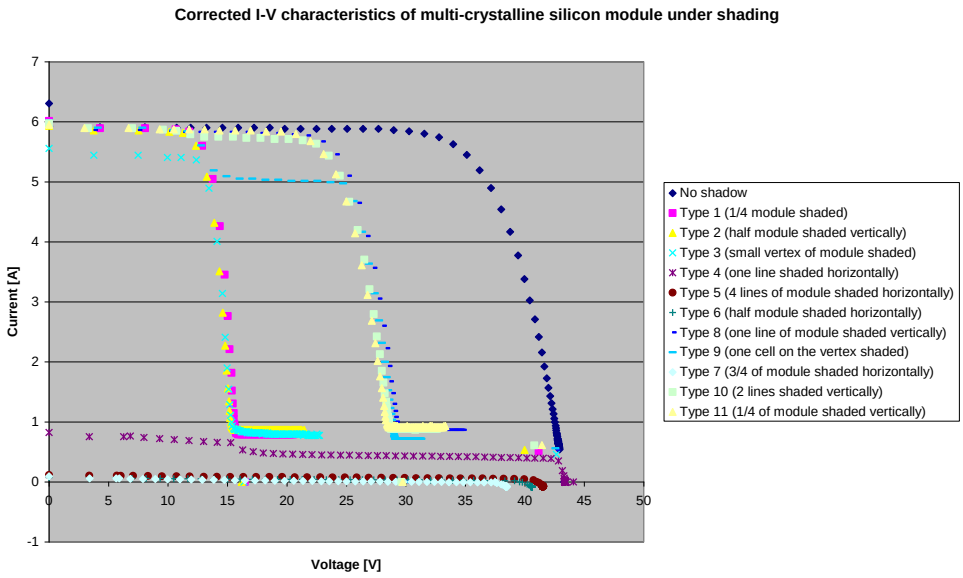

Fig. 6.17. Corrected I-V characteristics of multicrystalline silicon module under shading

The unshaded multicrystalline silicon module was taken as a reference and it produced the highest electrical characteristics (current, voltage and maximum power) compared to the shadow patterns. The analysis of the shadow patterns shows that type 8 produced the highest electrical characteristics and type 7 produced the lowest electrical characteristics.

The figure 6.17 above indicates that the mc-Si module has only 2 bypass diodes. The 2 bypass diodes were activated by the type 9 shadow only. The following shadow patterns activated one bypass diode only; type 8, type 10, type 11, type 1, type 2, type 3 and type 4. The rest of the shadow patterns did not activate the bypass diodes and they had lower electrical characteristics than the shadow patterns which activated the bypass diodes.

The shadow pattern and the location of the bypass diodes in the module influence the electrical characteristics of the module. The electrical characteristics do not directly depend on the shadow area because small shadow areas may produce high electrical characteristics because of the cell and bypass diode arrangement in the module. In general, shading reduces the electrical characteristics of the multicrystalline silicon module.

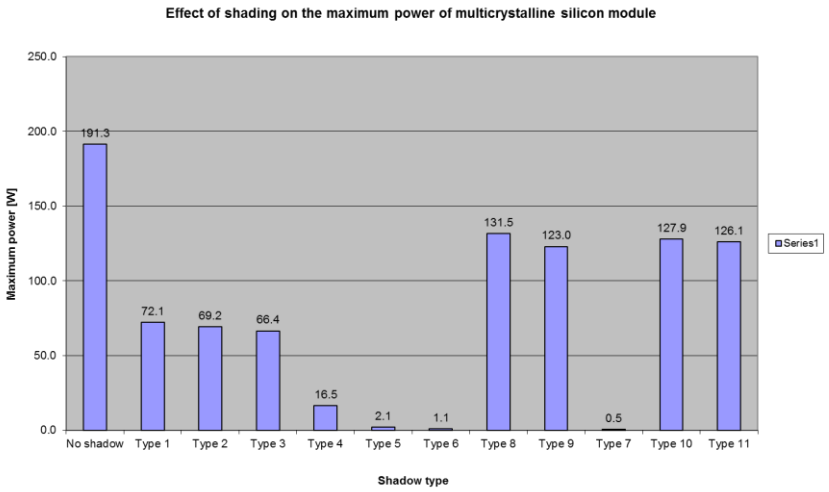

Fig. 6.18. Effect of shading on the maximum power of multicrystalline silicon module

The reference module (unshaded module) produced the highest maximum power (191.3 W). Among the shadow patterns, type 8 produced the highest maximum power (131.5 W) and type 7 produced the lowest maximum power (0.5 W).

The figure 6.18 above shows that shading reduces the maximum power of the mc-Si module. The magnitude of the maximum power depends on the shadow pattern, arranged of the cells in the module and the location of the bypass diodes.

Therefore, shading should be avoided in order to produce the highest maximum power in the multi-crystalline silicon module.

6.2 Thermal characteristics of the PV modules under shading

The results of the thermal characteristics of the PV module technologies indicate that shadow patterns resulted into reduction of the temperature of the modules. The Infrared (IR) thermograph results indicate that there were no hot spots in all the module technologies tested.

Some of the IR thermograph results have been inserted in the report and the rest were left since there were no significant differences in the results. For each module, shading reduced the module temperature and there were no hot spots formed.

One shadow type has been considered for each module in the report and selection of the shadow types was random. The selection was based on ensuring that most of the shadow types are represented in the report.

Cadmium Telluride (CdTe)

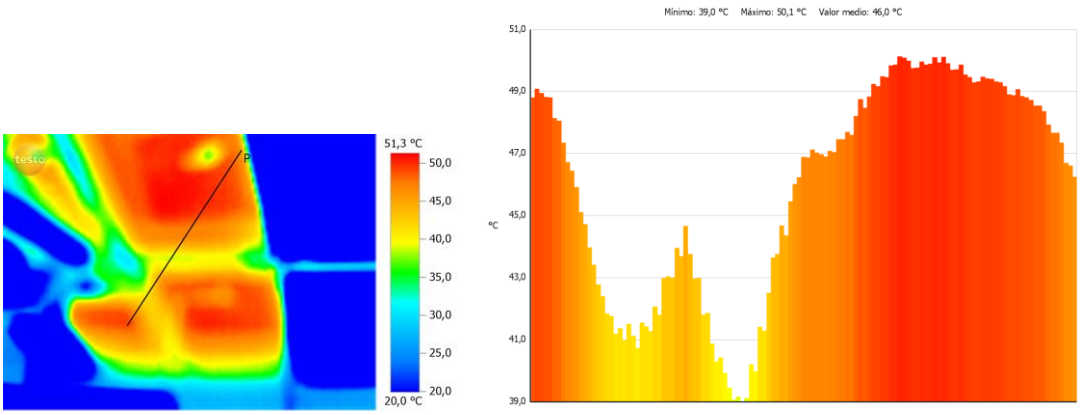

(a) (b)

Fig. 6.19. Temperature of the CdTe module under no shading; *(a) module, (b) Temperature profile*

The figure 6.19 above indicates that there was a small variation in the module temperature when shading is not applied on the CdTe module. The module temperature lied between 39.0 ^{o}C and 50.1 ^{o}C. Non uniform temperature across the module could be due to mismatch between PV cells, the proximity of junction-boxes or module frames.

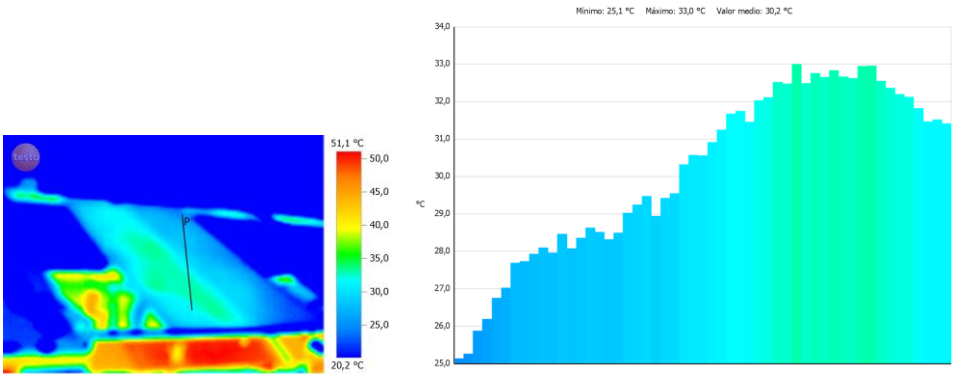

(a) (b)

Fig. 6.20. Temperature of the top of the CdTe module under type 2 shadow; *(a) Temperature distribution, (b) Temperature profile*

The type 2 shadow caused the variation of the module temperature distribution as shown in the figure 6.20 above. The module temperatures on top of the module lied between 25.1 ^{o}C and 33.0 ^{o}C. The module temperature measurements on top of the module were not accurate because of the reflection of the sun´s radiation. The part of the module which was shaded had lower temperatures than the unshaded part. There was no hot spot formation in the module under shading since module temperatures of the shaded part were lower than the unshaded part of the module. The module temperature measurements for the all the shadow patterns applied on the CdTe module indicate module temperature reduction during shading and no hot spot formation. In general, the shading of the CdTe module reduced the module temperatures compared to the unshaded module and there were no hot spots.

Copper indium selenide (CIS)

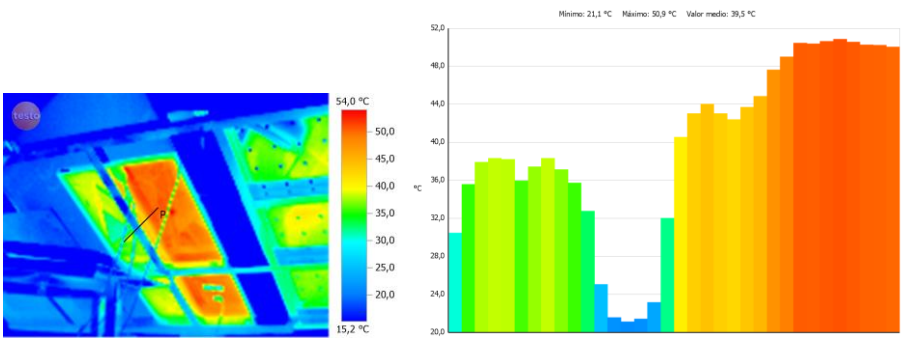

(a) (b)

Fig. 6.21. Temperature of CIS module under type 2 shadow; *(a) Temperature distribution, (b) Temperature profile*

The figure 6.21 above shows that type 2 shadow did not cause any hot spots in the CIS module. The module temperature under the type 2 shadow was between 30 ^{o}C and 40 ^{o}C. The temperature of the unshaded part lied between 40 ^{o}C and 50.9 ^{o}C. All the shadow patterns subjected to the CIS module indicate that there was a reduction in the module temperature by shading and there were no hot spots in the module. Therefore, shading reduced the module temperatures of CIS module and there were no hot spots in the module.

Amorphous silicon (a-Si) heterojunction

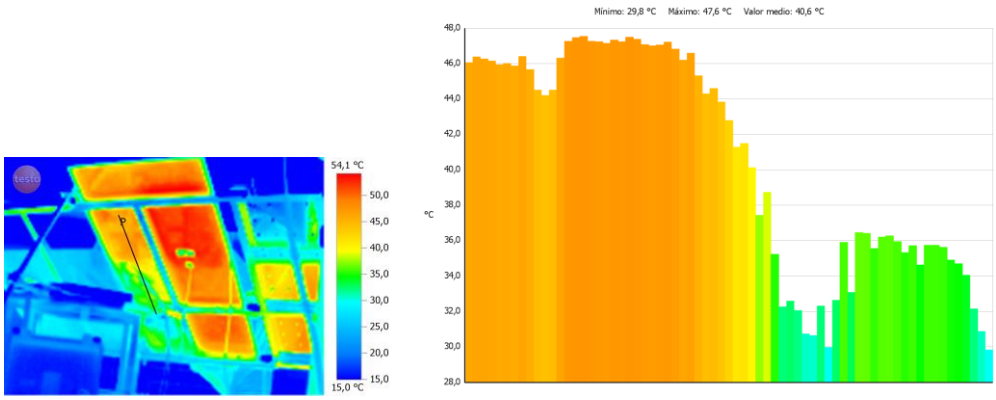

(a) (b)

Fig. 6.22. Temperature of a-Si heterojunction module type 1 shadow; *(a) Temperature distribution, (b) Temperature profile*

The above figure 6.22 shows the module temperature distribution for the a-Si heterojunction module subjected to type 1 shadow. The module temperature of the shaded part of the module was lower than the unshaded part. The temperature of the module under the type 1 shadow lied between 30 ^{o}C and 40 ^{o}C. The module temperature under the unshaded part was between 40 ^{o}C and 47.6 ^{o}C. The results of all the shadow patterns on the module indicate module temperature reduction for the shaded part of the module when compared to the unshaded part.

Amorphous silicon (Si-a) simple junction

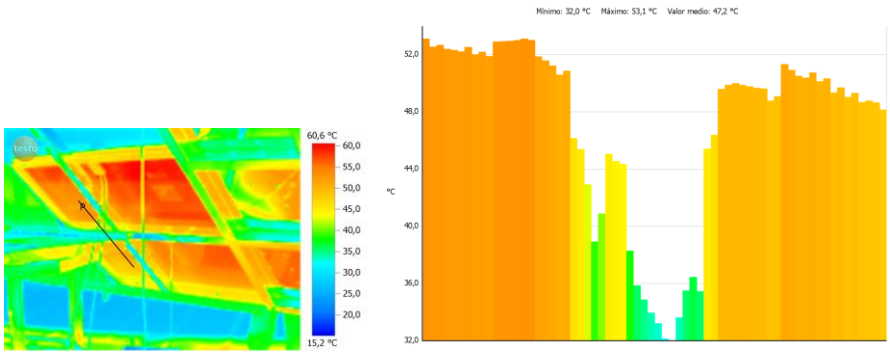

(a) (b)

Fig. 6.23. Temperature distribution of a-Si simple junction module type 6 shadow; *(a) Temperature distribution, (b) Temperature profile*

The module temperatures of the shaded parts of the a-Si simple junction module were lower than the module temperatures of the shaded part. There were no hot spots in the a-Si module considering all the shadow patterns applied on it.

The figure 6.23 above indicates the module temperature distribution for type 6 shadow. The module temperatures for the module subjected to type 6 shadow were lower than the unshaded part. The module temperatures for the type 6 shadow were between 43 ^{o}C and 50 ^{o}C. The module temperatures for the unshaded part were between 50 ^{o}C and 53.1 ^{o}C.

Amorphous silicon (a-Si) triple junction

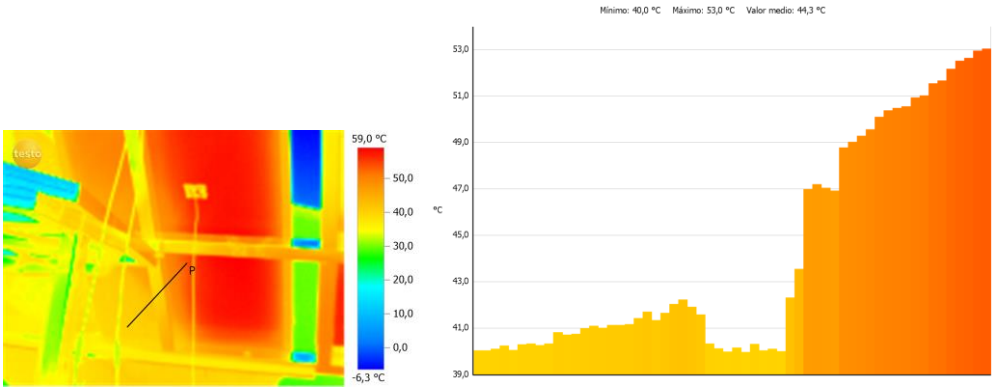

(a) (b)

Fig. 6.24. Temperature of a-Si triple junction module under type 3 shadow; *(a) Temperature distribution, (b) Temperature profile*

The module temperatures of the shaded parts of the a-Si triple junction module were generally lower than the unshaded parts for all the shadow patterns subjected to the module. There were also no hot spots in the module for all shadow patterns applied on the module.

The figure 6.24 above shows the temperature distribution of the a-Si triple junction module for the type 3 shadow. The module temperatures for the type 3 shadow were lower than the unshaded part and there were no hot spots in the module. The module temperatures for the shaded part lied between 35 ^{o}C and 45 ^{o}C. The module temperatures for the unshaded part lied between 45 ^{o}C and 53 ^{o}C.

Mono-crystalline silicon (m-Si)-Kyocera

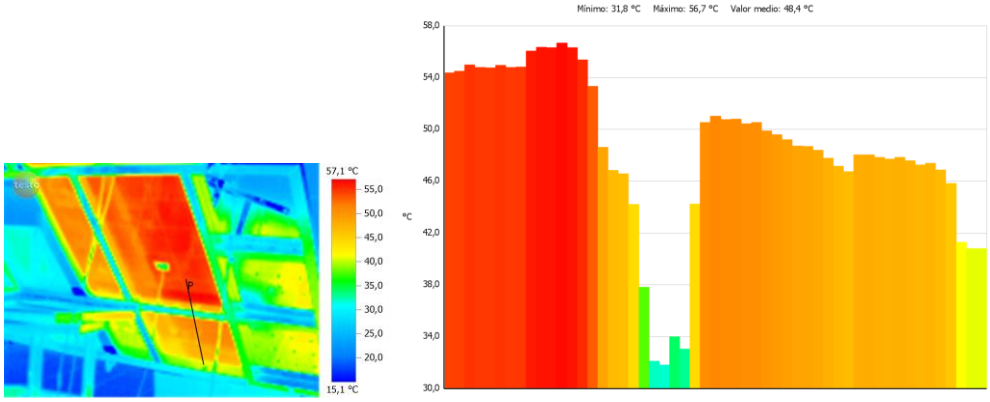

(a) (b)

Fig. 6.25. Temperature of m-Si module (Kyocera) under type 5 shadow; *(a) Temperature distribution, (b) Temperature profile*

The module temperatures for all the shadow patterns of monocrystalline silicon module were lower than the unshaded parts of the module and there were no hot spots.

The figure 6.25 above indicates the module temperature distribution for the type 5 shadow pattern. The module temperatures of the shaded part of the module were lower than the unshaded part. The module temperatures of the shaded part were between 40 ^{o}C and 45 ^{o}C. The module temperatures for the unshaded part were between 45 ^{o}C and 56.7 ^{o}C.

Mono-crystalline silicon (m-Si)-Suntech

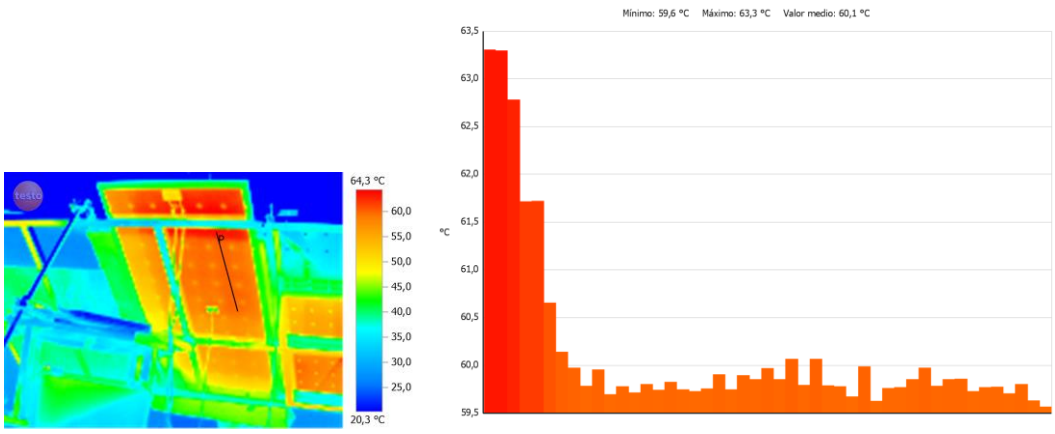

Fig. 6.26. Temperature of m-Si module (Suntech) under type 7 shadow; *(a) Temperature distribution, (b) Temperature profile*

The module temperatures for all the shadow patterns of monocrystalline silicon module (Suntech) were lower than the unshaded parts of the module and there were no hot spots.

The figure 6.26 above indicates the module temperature distribution and temperature profile for the type 7 shadow pattern. The module temperatures of the shaded part of the module were lower than the unshaded part. The module temperatures of the shaded part were between 47 ^{o}C and 55 ^{o}C. The module temperatures for the unshaded part were between 55 ^{o}C and 63.3 ^{o}C.

Mono-crystalline silicon (Si-m) back contacts

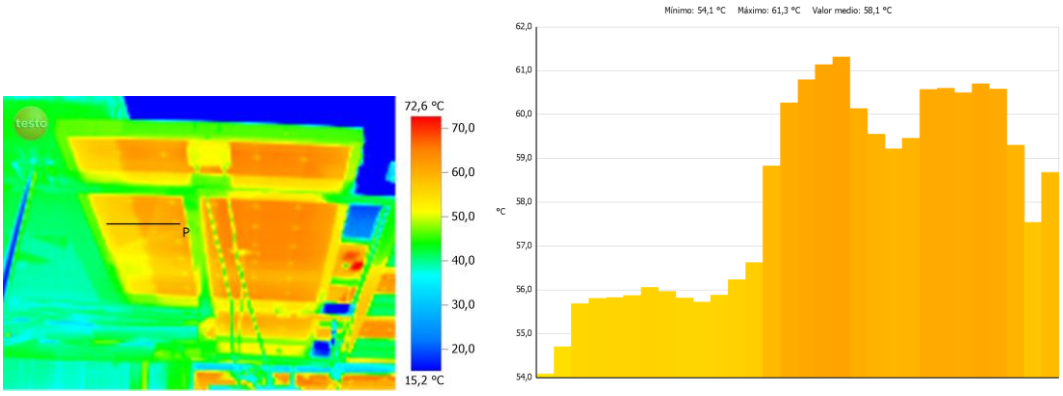

(a) (b)

Fig. 6.27. Temperature of monocrystalline silicon back contacts module type 4 shadow; *(a) Temperature distribution, (b) Temperature profile*

The figure 6.27 above shows the module temperature distribution of the monocrystalline silicon back contacts module subjected to type 4 shadow. The module temperatures of the shaded part of the module (50-57 ^{o}C) were lower than the unshaded part (57-61.3 ^{o}C) and there were no hot spots. The module temperatures of the shaded parts the m-Si back contacts module for all the shadow patterns were lower than the un shaded parts and there were no hot spots.

Multi-crystalline silicon (Si-mc)

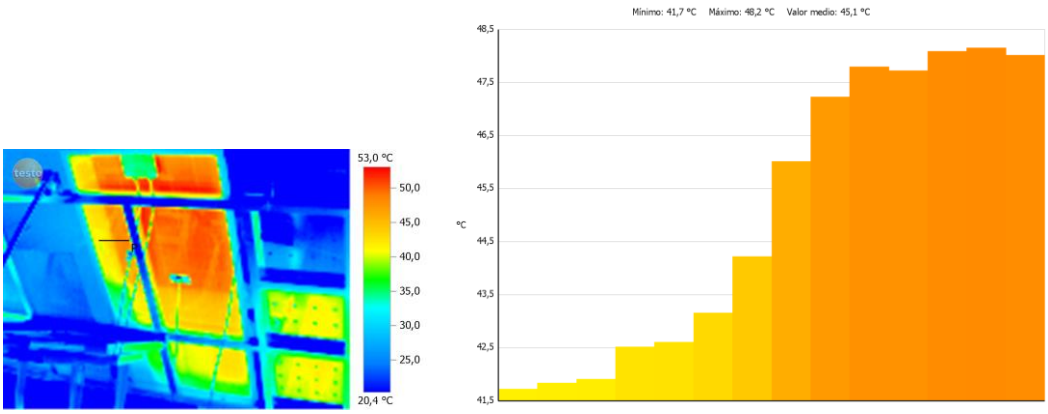

(a) (b)

Fig. 6.28. Temperature of multicrystalline silicon module type 8 shadow; *(a) Temperature distribution, (b) Temperature profile*

The module temperatures of shaded parts of the multi-crystalline silicon module for all the shadow patterns were lower than the unshaded parts and there were no hot spots.

The above figure 6.28 shows the module temperature distribution and temperature profile for the type 8 shadow subjected on the mc-Si module. The module temperatures of the shaded part (40-44 ^{o}C) were lower than the unshaded part (44-48.2 ^{o}C) and there were no hot spots.

6.3 Internal series resistance (R_s) and curve correction factor (k)

The internal series resistance (R_s), curve correction factor (k), alpha and Beta were used to correct the I-V curves to the same conditions. The environmental conditions also vary and correction of the electrical results makes it easier to compare the electrical characteristics of the modules.

The table 6.10 below shows the Rs, k, alpha and Beta values that were used to determine electrical characteristics of the PV modules.

Table. 6.2. R_s and k for the PV module technologies

Module technology	**Alpha (mA/^{o}C)**	**Beta (mV/^{o}C)**	**R_s (ohm)**	**K (ohm/^{o}C)**
CdTe	0.75	-166.6	2.89	-0.0164
CIS	1.25	-127.6	0.71	-5.00E-03
a-Si heterojunction	2.21	-109	0.76	5.00E-03
a-Si simple junction	0.89	-285.2	18.9	-1.18E-01
a-Si triple junction	5.1	-0.008	0.82	8.75E-03
m-Si (Kyocera)	4.98	-0.12	0.76	1.70E-02
m-Si (Suntech)	0.88	-150.3	1.58	1.40E-02
m-Si back contacts	3.5	-0.133	1.41	3.96E-02
mc-Si	4.32	-141.184	1.43	1.10E-02

The R_s and k values corrected the I-V curves of all the modules to the same conditions of irradiance and temperature. I-V curves correction made easier the comparison of shadow patterns for each module technology and comparison of the different module technologies under shading.

In the figures below, the I-V curves correction using R_s and k for Cadmium Telluride module has been presented.

Cadmium Telluride (CdTe)

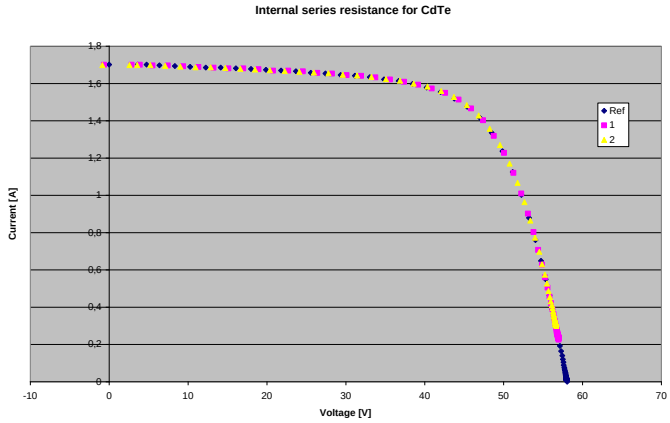

Fig. 6.29. Corrected I-V characteristics using the internal series resistance (R_s)

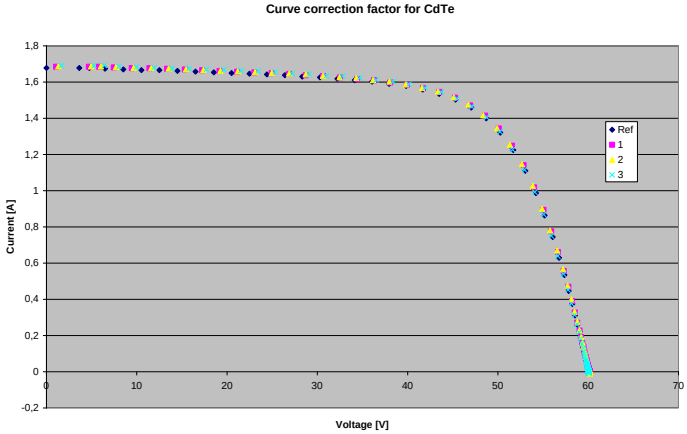

Fig. 6.30. Corrected I-V characteristics of CdTe module using curve correction factor (k)

6.4 Comparison of the different PV module technologies with shading

The behavior of the different PV module technologies under the same shadow patterns was compared. The maximum power of the PV module technologies was converted to standard test conditions (STC) for easier comparison since the environmental conditions always vary. The experiments were done on different days and there were always varying environmental conditions such as irradiance, ambient temperature, wind conditions. The environmental conditions affect the module temperature variation under different irradiance conditions. The application of shadow patterns on the modules depended on the arrangement of cells in the modules and not all modules were exposed to all the 11 shadow patterns.

The unshaded modules were taken as the reference and the variation of the maximum power at STC of the different PV module technologies under shading from the reference was analysed. The results indicate that the PV module technologies behave differently when subjected to the same shadow patterns.

Type 1 shadow

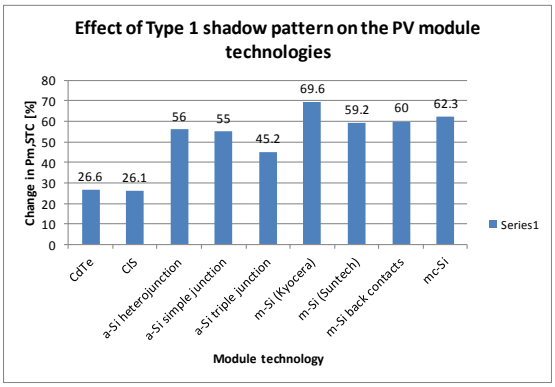

Fig. 6.31. Effect of type 1 shadow on the PV module technologies

The figure 6.31 above indicates that Copper indium selenide (CIS) module was least affected by type 1 shadow since it had the lowest variation of maximum power at STC from the reference (26.1%). Monocrystalline silicon (Kyocera) was the most affected module under type 1 shadow because it had the highest variation of the maximum power at STC from the reference (69.6%).

The Cadmium Telluride (CdTe) also performed well under type 1 shadow and the variation of the maximum power at STC from the reference (26.6%) was very close the CIS module.

Therefore, in real operating conditions of building integrated photovoltaics (BIPV) where shadows similar to type I shadow pattern are frequent, it is good to install CIS or CdTe module technologies.

Type 2 shadow

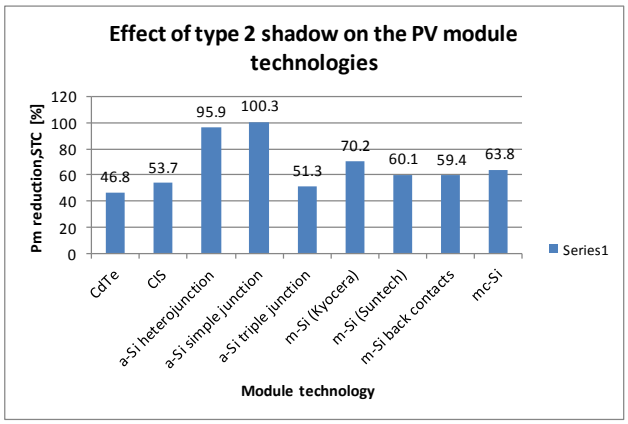

Fig. 6.32. Effect of type 2 shadow on the PV module technologies

The figure 6.32 above shows the effect of type 2 shadow pattern on the different PV module technologies. Cadmium Telluride (CdTe) module performed best under type 2 shadow since it had the lowest variation of maximum power at STC from the reference (46.8%) and amorphous silicon (a-Si) simple junction module performed worst since it had the highest variation of maximum power at STC from the reference (100.3%).

The a-Si tripple junction and CIS module also performed well under type 2 shadow with the maximum power variation at STC from the reference of 51.3% and 53.7% respectively. In general, it is recommended to install any of the following module technologies in building integrated photovoltaics (BIPV); CdTe, a-Si tripple junction and CIS in places where shadows similar to type 2 shadow pattern are frequent.

Type 3 shadow

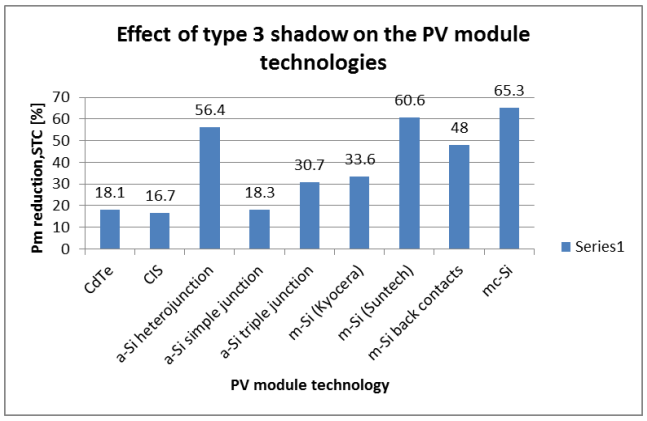

Fig. 6.33. Effect of type 3 shadow on the PV module technologies

The CIS module perfomed best under type 3 shadow with the lowest maximum power variation from reference of 16.7% and multicrystalline silicon module (mc-Si) performed worst with the highest maximum power variation from the reference of 65.3% as shown in the figure 6.33 above.

Cadmium Telluride (CdTe) and amorphous silicon (a-Si) simple junction modules also performed well under type 3 shadow pattern with the maximum power variation at STC from the reference of 18.1% and 18.3% respectively. Therefore, in the application of building integrated photovoltaics (BIPV) where the shadows similar to type 3 shadow pattern are frequent, it is recommended to install one of the following module technologies; CIS, CdTe and a-Si simple junction.

Type 4 shadow

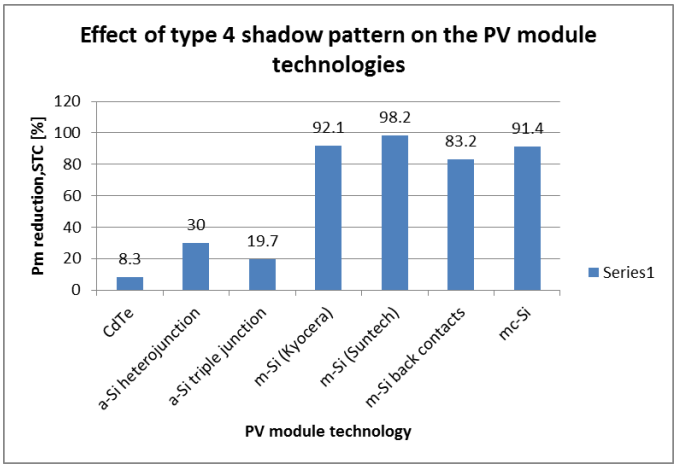

Fig. 6.34. Effect of type 4 shadow on the PV module technologies

The figure 6.34 above indicates the effect of type 4 shadow pattern on the different PV module technologies. Cadmium Telluride (CdTe) module performed best under type 4 shadow pattern since it had the lowest maximum power variation at STC from the reference of 8.3% and monocrystalline silicon (m-Si)-Suntech performed worst with the highest maximum power variation at STC from the reference of 98.2%.

Amorphous silicon (a-Si) tripple junction and amorphous silicon (a-Si) heterojunction modules also performed well compared to the rest of the PV module technologies with the maximum power variation at STC from the reference of 19.7% and 30% respectively. In general, in the application of building integrated photovoltaics where shadows similar to type 4 shadow are common, it is recommended to install one of the following technologies; CdTe, a-Si tripple junction and a-Si heterojunction.

Type 5 shadow

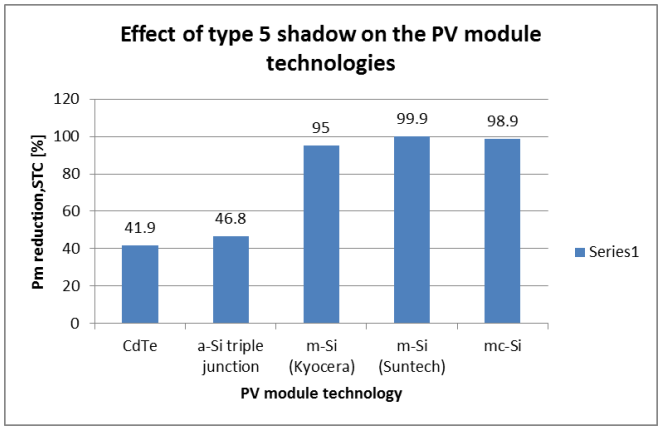

Fig. 6.35. Effect of type 5 shadow on the PV module technologies

The Cadmium Telluride (CdTe) module performed best under type 5 shadow pattern with the lowest maximum power variation at STC from reference of 41.9% and monocrystalline silicon (m-Si)-Suntech perfomed worst with the highest maximum power variation at STC from the reference of 99.9%.

Amorphous silicon (a-Si) triple junction module also performed well under type 5 shadow pattern with the maximum power variation from the reference of 46.8%. Therefore, in places where shadows similar to type 5 shadow pattern are frequent, it is recommended to install either CdTe or a-Si triple junction module technologies in building integrated photovoltaics (BIPV).

Type 6 shadow

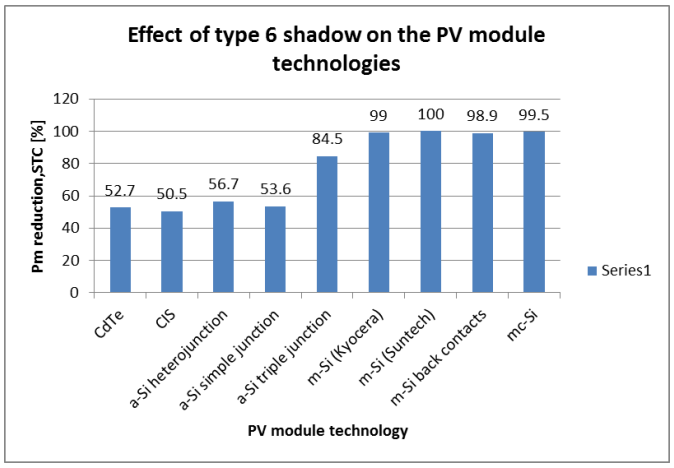

Fig. 6.36. Effect of type 6 shadow on the PV module technologies

The figure 6.36 above shows the effect of type 6 shadow pattern on the different PV module technologies. Copper indium selenide (CIS) module performed best under type 6 shadow with the lowest maximum power variation from the reference of 50.5% and monocrystalline silicon (m-Si) performed worst with the highest maximum power variation at STC from the reference of 100%.

Cadmium Telluride (CdTe), amorphous silicon (a-Si) simple junction and a-Si heterojunction module technologies also performed well under type 6 shadow with the maximum power variation at STC from the reference of 52.7%, 53.6% and 56.7% respectively. In the application of Building integrated photovoltaics (BIPV) where shadows similar to type 6 shadow pattern are common, it is recommended to install any of the following module technologies; CIS, CdTe, a-Si simple junction and a-Si heterojunction.

Type 7 shadow

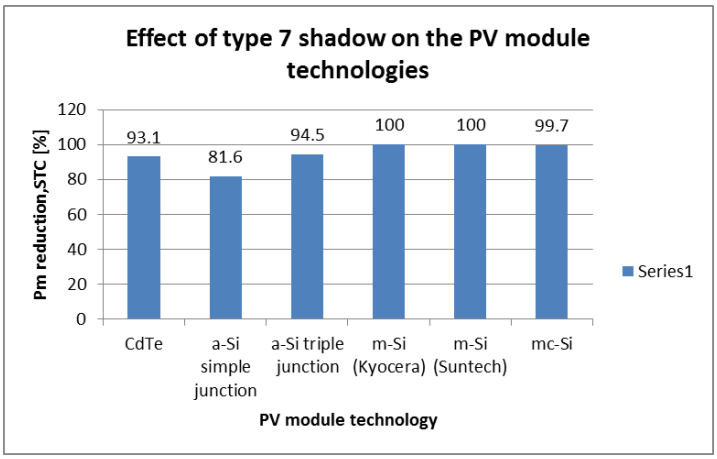

Fig. 6.37. Effect of type 7 shadow on the PV module technologies

The type 7 shadow greatly affected all the PV module technologies because the maximum power variation at STC from the reference was more than 80% as shown in the figure 6.37 above. The amorphous silicon (a-Si) simple junction module technology performed best with the lowest maximum power variation at STC from the reference of 81.6%. Monocrystalline (m-Si)-Kyocera and m-Si (Suntech) had the least maximum power variation at STC from the reference of 100%. In real situations where shadows similar type 7 shadow pattern are frequent, it is good to install a-Si simple junction during Building integrated photovoltaics (BIPV).

Type 8 shadow

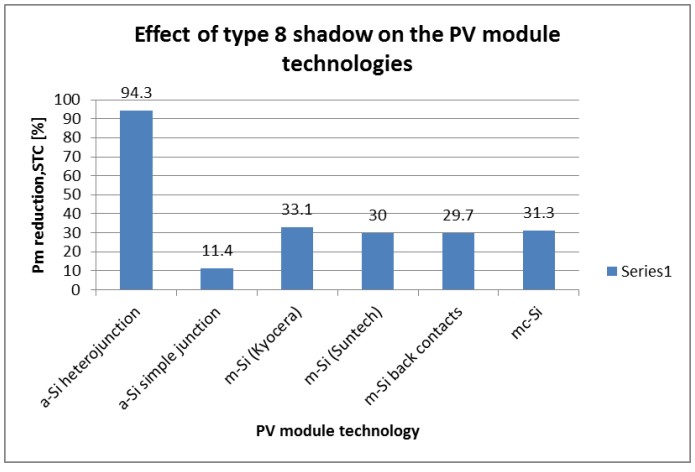

Fig. 6.38. Effect of type 8 shadow on the PV module technologies

The figure 6.38 above shows the maximum power variation at STC from the reference of the different PV module technologies under type 8 shadow. Amorphous silicon (a-Si) simple junction module performed best with the lowest maximum power variation at STC from the reference of 11.4% and a-Si heterojunction module performed worst with the highest maximum power variation at STC from the reference of 94.3%.

Monocrystalline silicon (m-Si) back contacts, m-Si (Suntech), multicrystalline silicon (mc-Si) and m-Si (Kyocera) also performed well under type 8 shadow with the maximum power variation at STC from the reference of 29.7%, 30%, 31.3% and 33.1% respectively. The following PV module technologies are suitable for application in Building integrated photovoltaics in places where shadows similar to type 8 shadow pattern are frequent; a-Si simple junction, m-Si back contacts, m-Si (Suntech), mc-Si and m-Si (Kyocera).

Type 9 shadow

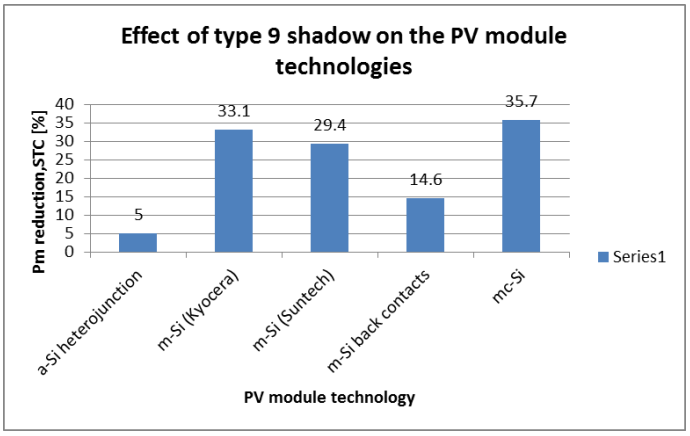

Fig. 6.39. Effect of type 9 shadow on the PV module technologies

Amorphous silicon (a-Si) heterojunction module performed best under type 9 shadow pattern with the lowest maximum power variation at STC from the reference of 5% and multicrystalline silicon (mc-Si) module performed worst with the highest maximum power variation at STC from the reference of 35.7%.

Monocrystalline silicon (m-Si) back contacts module also performed well under type 9 shadow with the maximum power variation at STC from the reference of 14.6%. In the selection of module technology to be installed in building integrated photovoltaics (BIPV) for a location where shadows similar to type 9 shadow pattern are frequent, it is recommeded to install either a-Si heterojuction or m-Si back contacts module technologies.

Type 10 shadow

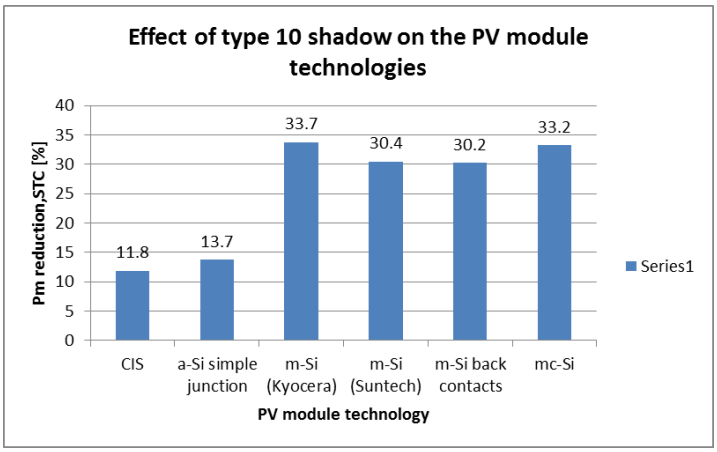

Fig. 6.40. Effect of type 10 shadow on the PV module technologies

The figure 6.40 above indicates the maximum power variation at STC from the reference under type 10 shadow pattern for the different PV module technologies as shown in figure 6.40 above. Copper indium selenide (CIS) module technology performed best with the lowest maximum power variation at STC from the reference of 11.8% and monocrystalline silicon (Kyocera) performed worst with the highest maximum power variation at STC from the reference of 33.7%.

Amorphous silicon (a-Si) simple junction also performed well under type 10 shadow with the maximum power variation at STC from the reference of 13.7%. Therefore, it is recommended to install either CIS or a-Si simple junction module technologies in Building integrated photovoltaics (BIPV) in locations where shadows similar to type 10 shadow pattern are common.

Type 11 shadow

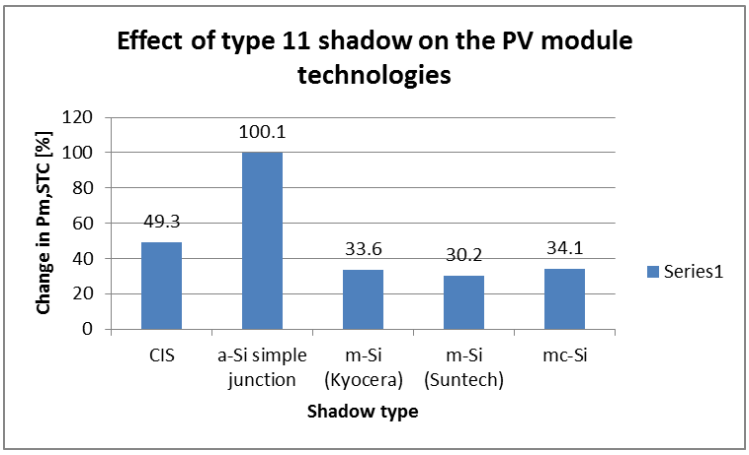

Fig. 6.41. Effect of type 11 shadow on the PV module technologies

Monocrystalline silicon (m-Si)-Suntech module technology performed best with the lowest maximum power variation at STC from the reference of 30.2% and amorphous silicon (a-Si) simple junction performed worst with the highest maximum power variation at STC from the reference of 100.1% as shown in the figure 6.41 above.

m-Si (Kyocera), multicrystalline silicon (mc-Si) and copper indium selenide (CIS) module technologies also performed well under type 11 shadow with the maximum power variation at STC from the reference of 33.6%, 34.1% and 49.3% respectively. In locations where shadows similar to type 11 shadow pattern, its recommended to employ the following module technologies in Building integrated photovoltaics (BIPV); m-Si (Suntech), m-Si (Kyocera), mc-Si and CIS.

CONCLUSIONS

The electrical and thermal characteristics of the PV module technologies is affected by shadows, mismatch effects. The variation of the electrical and thermal characteristics is mostly caused by shading.

The analysis of the different PV module technologies indicates that shading causes the reduction of the electrical characteristics (current, voltage and power). For every shadow pattern, the I-V characteristics reduced when compared to the unshaded module (reference). The magnitude of the reduction of the electrical characteristics of the PV modules by shading does not directly depend on the shading area but depends on the cells orientation, number of cells and location of bypass diodes in the module. The shadow area may be small but cause higher reduction of the electrical parameters than a big shadow if for example the former does not have bypass diodes and if the latter has them.

The thermal characterisation indicates that shading resulted into the reduction of the module temperatures in comparison to the unshaded module and there were no hot spots in all the module technologies during the time the measurements were taken. Therefore, all the module technologies tested are capable of being applied in building integrated photovoltaics (BIPV) since they are not affected by hot spot phenomena in the real operating conditions.

The comparison of the different PV module technologies with the same shadow patterns indicate that the modules perform differently with shading. For each shadow type, the best module technologies with the lowest maximum power variation at STC from the reference and the worst module technologies with the highest maximum power variation at STC from the reference were obtained. The results indicate that some PV module technologies which perform well in one shadow pattern do not perform well in another shadow pattern.

In the application of BIPV in buildings, shading should be taken as a priority since it greatly affects the electrical and thermal characteristics of the modules. The nature of the shadows in a location should be considered before selecting the PV module technologies to apply in the BIPV system and deciding the position of the module in the building.

RECOMMENDATIONS

This research topic focussed on the study of shading in building integrated photovoltaics (BIPV) where the electrical and thermal characterisation were carried out. There are other factors that affect the performance of the PV modules in BIPV such as mismatch effects.

PV modules for application in BIPV should have the electrical, thermal, mechanical and water drainage properties for suitability in electrical power production and construction purposes.

I recommend further research on the following areas;

- **Mismatch effects of photovoltaic module technologies in BIPV**; Mismatch also affects the electrical and thermal properties of the PV modules. This could differentiate the effects of mismatch effects from the effects of shading in BIPV.

- **Drainage properties of photovoltaic module technologies in BIPV**; This is very important for the building during the rainy seasons. The building should have the capacity to drain the water during raining period and prevent water from entering the interior of the building.

- **Mechanical strength of photovoltaic module technologies in BIPV**; The buildings are subjected to different loads such as wind loads which could affect the performance of BIPV. The PV modules should be strong to withstand all the loads subjected to the building.

REFERENCES

[1] Scognamiglio. A and Privato. C. Starting points for a new cultural vision of BIPV. Proceedings of the 23rd European Photovoltaic Solar Energy Conference, 1-5 September 2008, Valencia, Spain

[2] European Photovoltaic Industry Association (EPIA). Solar photovoltaics competing in the Energy sector. On the road to competitiveness, September 2011. www.epia.org, accessed in July 2013.

[3] Jiang F., Khaing H and Liang Y. J. Performance of BIPV Systems under Shadows. Proceedings of the 2012 International Congress on Informatics, Environment, Energy and Applications-IEEA 2012 IPCSIT vol.38 (2012) © (2012) IACSIT Press, Singapore.

[4] Silvestre S and Chouder A. Effects of Shadowing on Photovoltaic Module Performance. Progress in Photovoltaics: Research and Publications. *Prog. Photovolt: Res. Appl. 2008; **16**:141-149.*

[5] Martín N., Alonso-García M.C., Chenlo F and Sánchez-Friera P. Electrical and thermal characterisation of PV modules under partial shadowing. Proceedings of the 23rd European Photovoltaic Solar Energy Conference, 1-5 September 2008, Valencia, Spain.

[6] Keith Emery. Measurement and Characterization of Solar Cells and Modules. National Renewable Energy Laboratory, Golden, CO, USA. Handbook of Photovoltaic Science and Engineering.

[7] Changhai P., Ying H., Zhishen W. Building integrated photovoltaics (BIPV) in architectural design in China. Energy and buildings 43 (2011) 3592-3598.

[8] Vorster F. J., Van Dyk E. E. Current-Voltage Characteristics of High-Concentration, Photovoltaic Arrays. Progress in Photovoltaics: Research and Applications. *Prog. Photovolt: Res. Appl. 2005; **13**:55-56*

[9] Ronald J.C and Zolingen V. Electrotechnical Requirements for PV on Buildings. Progress in Photovoltaics: Research and Applications. *Prog. Photovolt: Res. Appl. 2004; **12**: 409-414 (DOI: 10. 1002/pip.557)*

[10] Munoz J., Lorenzo E., Martinez-Moreno F., Marroyo L and Garcia M. An Investigation into Hot-Spots in Two Large Grid-Connected PV Plants. Progress in Photovoltaics: Research and Applications. *Prog. Photovolt: Res. Appl. 2008; **16**: 693-701*

[11] Duran E., Andujar J. M., Galan J and Sidrach-de-Cardona M. Methodology and Experimental System for Measuring and Displaying I-V Characteristic Curves of PV Facilities. Progress in Photovoltaics: Research and Applications. *Prog. Photovolt: Res. Appl. 2009; **17**: 574-586*

[12] Martinez-Moreno F., Lorenzo E., Munoz J., and Moreton R. On the testing of large PV arrays. Progress in Photovoltaics: Research and Applications. *Prog. Photovolt:*

*Res. Appl. 2012; **20**: 100-105.*

[13] Alonso Garcia M. C., Herrmann W., Bohmer W and Proisy B. Thermal and Electrical Effects Caused by Outdoor Hot-spot Testing in Associations of Photovoltaic Cells. Progress in Photovoltaics: Research and Applications. *Prog. Photovolt: Res. Appl. 2003; **11**: 293-307.*

[14] Alonso-Garcia M. C., Ruiz J. M and Chenlo F. Experimental study of mismatch and shading effects in the I-V characteristic of a photovoltaic module. Solar energy materials & solar cells 90 (2006) 329-340.

[15] Alonso-Garcia M.C., Ruiz J. M and Herrmann W. Computer simulation of shading effects in photovoltaic arrays. Renewable Energy 31 (2006) 1986-1993.

[16] Alonso-Garcia M.C., Chenlo F., Sanchez-Friera P. Experimental results on module characterization for hot-spot protection. Technical Digest for the International PVSEC-17, Fukuoka, Japan, 2007.

[17] Vardoulakis E., Karamanis D. The effect of shading of building integrated photovoltaics on roof surface temperature and heat transfer in buildings. *Proceedings of ECOS 2012-The 25th International conference on efficiency, cost, optimization, simulation and environmental impact of energy systems, June 26-29, 2012, Perugia, Italy.*

[18] Elhassan Z. A. M., Mohd Zain M. F., Sopian K and Abass A. A. Building integrated photovoltaics (BIPV) module in urban housing in Khartoum: Concept and design considerations. *International Journal of the Physical Sciences Vol. 7(3), pp. 487-494, 16 January 2012.*

[19] Solar efficiency chart. http://solartribune.com/wp-content/uploads/2011/07/nrel.gov-solar-cells-efficiency.jpg, accessed in August 2013.

[20] Silvestre S., Boronat A and Chouder A. Study of bypass diodes configuration on PV modules. *Applied Energy 86 (2009) 1632-1640.*

[21] Mermoud A and Lejeune T. Partial shadings on PV arrays: Bypass diode benefits analysis. *25th European Photovoltaic Solar Energy Conference and Exhibition/ 5th World Conference on Photovoltaic Energy Conversion, 6-10 September 2010, Valencia, Spain.*

[22] Munro D. Lessons learnt from photovoltaics in urban areas. *23rd European Photovoltaic Solar Energy Conference, 1-5 September 2008, Valencia, Spain.*

[23] Imamura M.S and Helm P. Photovoltaic System Technology. A European Handbook for Commission of the European Communities. *Published by H S Stephens & Associates, Pavenham Road, Felmersham, Bedford MK43 7EX, England. Copy right 1992 ECSC, EEC, EAEC, Brussels and Luxembourg. ISBN 0-9510271-9-0*

APPENDIX

Maximum power at STC for different technologies under shading

Shadow type	Module technology	P_m [W]	G [W/m^2]	T (^{o}C)	Gamma	$P_{m,STC}$ [W]	Change in P_m, STC [%]
No shadow (Reference)	CdTe	84.96	835.96	31.8	-0.0025	103.4	
	CIS	88.38	905.13	23.6	-0.0036	97.2	
	a-Si heterojunction	254.15	902.15	29	-0.0030	285.1	
	a-Si simple junction	67.02	820.95	34.9	-0.0023	83.5	
	a-Si triple junction	67.63	866.96	30.5	-0.0021	78.9	
	m-Si (Kyocera)	218.416	887.58	28.6	-0.0046	250.2	
	m-Si (Suntech)	197.02	830.94	35	-0.0048	249.1	
	m-Si back contacts	261.52	852.64	26.1	-0.0038	308.0	
	mc-Si	191.31	851.8	27.2	-0.0043	226.7	
Type 1	CdTe	62.4	835.96	31.8	-0.0025	75.9	26.6
	CIS	65.35	905.13	23.6	-0.0036	71.8	26.1
	a-Si heterojunction	111.89	902.15	29	-0.0030	125.5	56.0
	a-Si simple junction	30.18	820.95	34.9	-0.0023	37.6	55.0
	a-Si triple junction	37.09	866.96	30.5	-0.0021	43.3	45.2
	m-Si (Kyocera)	66.31	887.58	28.6	-0.0046	76.0	69.6
	m-Si (Suntech)	80.4	830.94	35	-0.0048	101.6	59.2
	m-Si back contacts	104.68	852.64	26.1	-0.0038	123.3	60.0
	mc-Si	72.07	851.8	27.2	-0.0043	85.4	62.3
Type 2	CdTe	45.23	835.96	31.8	-0.0025	55.0	46.8
	CIS	40.89	905.13	23.6	-0.0036	44.9	53.7
	a-Si heterojunction	10.41	902.15	29	-0.0030	11.7	95.9
	a-Si simple junction	-0.19	820.95	34.9	-0.0023	-0.2	100.3
	a-Si triple junction	32.92	866.96	30.5	-0.0021	38.4	51.3
	m-Si (Kyocera)	65.008	887.58	28.6	-0.0046	74.5	70.2
	m-Si (Suntech)	78.6	830.94	35	-0.0048	99.4	60.1
	m-Si back contacts	106.19	852.64	26.1	-0.0038	125.1	59.4
	mc-Si	69.16	851.8	27.2	-0.0043	82.0	63.8
Type 3	CdTe	69.62	835.96	31.8	-0.0025	84.7	18.1
	CIS	73.61	905.13	23.6	-0.0036	80.9	16.7
	a-Si heterojunction	110.93	902.15	29	-0.0030	124.5	56.4
	a-Si simple junction	54.78	820.95	34.9	-0.0023	68.3	18.3
	a-Si triple junction	46.85	866.96	30.5	-0.0021	54.7	30.7
	m-Si (Kyocera)	145.117	887.58	28.6	-0.0046	166.3	33.6
	m-Si (Suntech)	77.56	830.94	35	-0.0048	98.0	60.6
	m-Si back contacts	135.87	852.64	26.1	-0.0038	160.0	48.0
	mc-Si	66.42	851.8	27.2	-0.0043	78.7	65.3
Type 4	CdTe	77.88	835.96	31.8	-0.0025	94.8	8.3

	CIS		905.13	23.6	-0.0036		
	a-Si heterojunction	177.92	902.15	29	-0.0030	199.6	30.0
	a-Si simple junction		820.95	34.9	-0.0023		
	a-Si triple junction	54.34	866.96	30.5	-0.0021	63.4	19.7
	m-Si (Kyocera)	17.272	887.58	28.6	-0.0046	19.8	92.1
	m-Si (Suntech)	3.54	830.94	35	-0.0048	4.5	98.2
	m-Si back contacts	43.9	852.64	26.1	-0.0038	51.7	83.2
	mc-Si	16.48	851.8	27.2	-0.0043	19.5	91.4
Type 5	CdTe	49.33	835.96	31.8	-0.0025	60.0	41.9
	CIS		905.13	23.6	-0.0036		
	a-Si heterojunction		902.15	29	-0.0030		
	a-Si simple junction		820.95	34.9	-0.0023		
	a-Si triple junction	35.98	866.96	30.5	-0.0021	42.0	46.8
	m-Si (Kyocera)	10.922	887.58	28.6	-0.0046	12.5	95.0
	m-Si (Suntech)	0.22	830.94	35	-0.0048	0.3	99.9
	m-Si back contacts		852.64	26.1	-0.0038		
	mc-Si	2.11	851.8	27.2	-0.0043	2.5	98.9
Type 6	CdTe	40.16	835.96	31.8	-0.0025	48.9	52.7
	CIS	43.74	905.13	23.6	-0.0036	48.1	50.5
	a-Si heterojunction	110.07	902.15	29	-0.0030	123.5	56.7
	a-Si simple junction	31.07	820.95	34.9	-0.0023	38.7	53.6
	a-Si triple junction	10.49	866.96	30.5	-0.0021	12.2	84.5
	m-Si (Kyocera)	2.206	887.58	28.6	-0.0046	2.5	99.0
	m-Si (Suntech)	0.09	830.94	35	-0.0048	0.1	100.0
	m-Si back contacts	2.9	852.64	26.1	-0.0038	3.4	98.9
	mc-Si	1.05	851.8	27.2	-0.0043	1.2	99.5
Type 7	CdTe	5.84	835.96	31.8	-0.0025	7.1	93.1
	CIS		905.13	23.6	-0.0036		
	a-Si heterojunction		902.15	29	-0.0030		
	a-Si simple junction	12.32	820.95	34.9	-0.0023	15.4	81.6
	a-Si triple junction	3.7	866.96	30.5	-0.0021	4.3	94.5
	m-Si (Kyocera)	-0.003	887.58	28.6	-0.0046	0.0	100.0
	m-Si (Suntech)	-0.07	830.94	35	-0.0048	-0.1	100.0
	m-Si back contacts		852.64	26.1	-0.0038		
	mc-Si	0.48	851.8	27.2	-0.0043	0.6	99.7
Type 8	CdTe		835.96	31.8	-0.0025		
	CIS		905.13	23.6	-0.0036		
	a-Si heterojunction	14.39	902.15	29	-0.0030	16.1	94.3
	a-Si simple junction	59.39	820.95	34.9	-0.0023	74.0	11.4
	a-Si triple junction		866.96	30.5	-0.0021		
	m-Si (Kyocera)	146.172	887.58	28.6	-0.0046	167.5	33.1
	m-Si (Suntech)	137.96	830.94	35	-0.0048	174.4	30.0

	m-Si back contacts	183.85	852.64	26.1	-0.0038	216.5	29.7
	mc-Si	131.5	851.8	27.2	-0.0043	155.9	31.3
Type 9	CdTe		835.96	31.8	-0.0025		
	CIS		905.13	23.6	-0.0036		
	a-Si heterojunction	241.4	902.15	29	-0.0030	270.8	5.0
	a-Si simple junction		820.95	34.9	-0.0023		
	a-Si triple junction		866.96	30.5	-0.0021		
	m-Si (Kyocera)	146.194	887.58	28.6	-0.0046	167.5	33.1
	m-Si (Suntech)	139.09	830.94	35	-0.0048	175.8	29.4
	m-Si back contacts	223.39	852.64	26.1	-0.0038	263.1	14.6
	mc-Si	122.97	851.8	27.2	-0.0043	145.7	35.7
Type 10	CdTe		835.96	31.8	-0.0025		
	CIS	77.92	905.13	23.6	-0.0036	85.7	11.8
	a-Si heterojunction		902.15	29	-0.0030		
	a-Si simple junction	57.82	820.95	34.9	-0.0023	72.1	13.7
	a-Si triple junction		866.96	30.5	-0.0021		
	m-Si (Kyocera)	144.747	887.58	28.6	-0.0046	165.8	33.7
	m-Si (Suntech)	137.05	830.94	35	-0.0048	173.2	30.4
	m-Si back contacts	182.59	852.64	26.1	-0.0038	215.0	30.2
	mc-Si	127.87	851.8	27.2	-0.0043	151.6	33.2
Type 11	CdTe		835.96	31.8	-0.0025		
	CIS	44.84	905.13	23.6	-0.0036	49.3	49.3
	a-Si heterojunction		902.15	29	-0.0030		
	a-Si simple junction	-0.04	820.95	34.9	-0.0023	0.0	100.1
	a-Si triple junction		866.96	30.5	-0.0021		
	m-Si (Kyocera)	145.054	887.58	28.6	-0.0046	166.2	33.6
	m-Si (Suntech)	137.52	830.94	35	-0.0048	173.8	30.2
	m-Si back contacts		852.64	26.1	-0.0038		
	mc-Si	126.05	851.8	27.2	-0.0043	149.4	34.1